

DTIC FILE COPY

AD-A222 952



THERMAL ANALYSIS  
OF HEAT PIPE RADIATORS WITH  
A RECTANGULAR GROOVE WICK STRUCTURE

THESIS

Chul Hwan Yang  
Major, ROKAF

AFIT/GA/ENY/90J-02

DISTRIBUTION STATEMENT A

Approved for public release;  
Distribution Unlimited

DEPARTMENT OF THE AIR FORCE  
AIR UNIVERSITY

**AIR FORCE INSTITUTE OF TECHNOLOGY**

Wright-Patterson Air Force Base, Ohio

90 06 20 062

DTIC  
ELECTE  
JUN 21 1990  
S E D

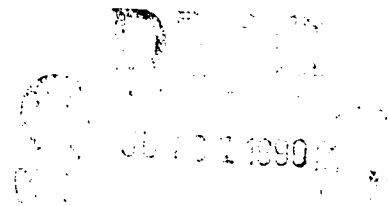
AFIT/GA/ENY/90J-02

THERMAL ANALYSIS  
OF HEAT PIPE RADIATORS WITH  
A RECTANGULAR GROOVE WICK STRUCTURE

THESIS

Chul Hwan Yang  
Major, ROKAF

AFIT/GA/ENY/90J-02



Approved for public release; distribution unlimited

AFIT/GA/ENY/90J-02

THERMAL ANALYSIS OF HEAT PIPE RADIATORS WITH A  
RECTANGULAR GROOVE WICK STRUCTURE

THESIS

Presented to the Faculty of the School of Engineering  
of the Air Force Institute of Technology  
Air University  
In Partial Fulfillment of the  
Requirements for the Degree of  
Master of Science in Astronautical Engineering

Chul Hwan Yang, B.S.

Major, ROKAF

June, 1990

Accession For	
NTIS	<input checked="checked" type="checkbox"/>
DTIC	<input checked="checked" type="checkbox"/>
Unpublished	<input type="checkbox"/>
Justification	
By	
Distribution/	
AFIT Policy Codes	
and/or	
Dist	Special
A-1	

Approved for public release; distribution unlimited

## *Acknowledgments*

I wish to express my profound gratitude to Capt. Daniel B. Fant, my thesis advisor, and Dr. Won Soon Chang, my thesis sponsor, for their continual guidance and encouragement, their careful reading of the original manuscript and their individual suggestions. I also wish to acknowledge Drs. James E. Hitchcock, and William C. Elrod, the members of my reading committee, for their kind review.

I would like to thank Capt. In-taek Kim who helped me write the FORTRAN program , and many others who helped me collect some of the materials for this thesis.

I would also like to thank Korea Air Force and my senior officers who gave me the opportunity to study in the United States.

Finally, I would like to express my appreciation to my wife and daughter for their sacrifices and encouragement that enabled me to complete this work.

Chul Hwan Yang

## *Table of Contents*

	Page
Acknowledgments . . . . .	ii
Table of Contents . . . . .	iii
List of Figures . . . . .	v
List of Tables . . . . .	vii
List of Symbols . . . . .	viii
Abstract . . . . .	xi
I. INTRODUCTION . . . . .	1-1
1.1 Background . . . . .	1-1
1.2 The Heat Pipe . . . . .	1-1
1.3 Objectives of the Study . . . . .	1-3
1.4 Literature Survey . . . . .	1-3
II. MATHEMATICAL ANALYSIS . . . . .	2-1
2.1 Heat Balance Equation . . . . .	2-1
2.1.1 Heat Pipe Section . . . . .	2-1
2.1.2 Heat Pipe Condenser Section with Fin . . . . .	2-9
2.2 Heat Transfer . . . . .	2-15
2.2.1 Fin Surface . . . . .	2-15
2.2.2 Total Surface . . . . .	2-15

	Page
III. COMPUTATIONAL PROCEDURE . . . . .	3-1
3.1 Summary of Equations and Finite Difference Forms . .	3-1
3.2 Initial Values . . . . .	3-3
3.3 Method of Calculation . . . . .	3-5
IV. RESULTS . . . . .	4-1
4.1 Heat Transfer Coefficient of Heat Pipe Radiator . . . .	4-1
4.1.1 Operating Temperature Effect: . . . . .	4-1
4.1.2 Heat Input Effect: . . . . .	4-1
4.2 Gray Surfaces with Negligible Fin thickness . . . . .	4-1
4.3 Heat pipe-Fin Radiator Efficiency . . . . .	4-9
V. CONCLUSION AND RECOMMENDATIONS . . . . .	5-1
Appendix A. FORTRAN PROGRAM . . . . .	A-1
Appendix B. VIEW FACTOR EQUATIONS . . . . .	B-1
B.1 View Factor from Fin to Heatpipe . . . . .	B-2
B.2 View Factor from Pipe to Pipe . . . . .	B-4
Appendix C. TABULATED RESULTS . . . . .	C-1
Appendix D. SIMPLE FIN SOLUTION . . . . .	D-1
Appendix E. PROPERTIES . . . . .	E-1
Bibliography . . . . .	BIB-1
Vita . . . . .	VITA-1

## *List of Figures*

Figure	Page
2.1. Multiple Heat Pipe Radiator in the Spacecraft . . . . .	2-2
2.2. The Cross-Sectional View of the Condenser Section of Heat Pipe Radiator . . . . .	2-3
2.3. Sketch of Heat Flow Path through a Single Heat Pipe . . . . .	2-4
2.4. Heat Flow Path in a Differential Fin Element . . . . .	2-10
4.1. Relationship between Radiation Parameter and Operating Temperature . . . . .	4-3
4.2. Total heat transfer rate of heat pipe vs. Operating Temperature .	4-4
4.3. Temperature Difference between Evaporator and Condenser Temperature vs. Operating Temperature . . . . .	4-5
4.4. Overall heat transfer coefficient of heat pipe vs. Operating Temperature . . . . .	4-6
4.5. Efficiency of Heat Pipe Radiator with Fin vs. Radiation Parameter	4-7
4.6. Condenser Surface Effects on Fin Heat Loss from Reference 14 .	4-8
4.7. Simple Fin Efficiency from Reference 14 . . . . .	4-9
4.8. Condenser Surface Heat Loss from Reference 14 . . . . .	4-10
B.1. Geometry Used in Fin-to-Heatpipe View Factor Determination . .	B-2
B.2. Geometry Used in Heatpipe-to-Heatpipe View Factor Determination	B-5
E.1. Thermal Conductivity of Pure Copper . . . . .	E-2
E.2. Density of Saturated Water ( Steam ) . . . . .	E-3
E.3. Latent Heat of Vaporization ( Water ) . . . . .	E-4
E.4. Viscosity of Water ( Steam ) . . . . .	E-5
E.5. Thermal Conductivity of Water ( Liquid ) . . . . .	E-6

### *List of Tables*

Table	Page
C.1. Characteristics of Radiator Parameter vs Condenser Temperature	C-2
C.2. Characteristics of temperature Difference and total heat transfer rate vs. Operating Temperature . . . . .	C-2
C.3. Characteristics of Heat Pipe vs. Operating Temperature . . . . .	C-3
C.4. Characteristics of Black Surface Heat Pipe Radiators with Fins of Negligible Thickness . . . . .	C-3
D.1. Charateristics of Simple Fin Radiators . . . . .	D-3



## *List of Symbols*

- $A_p$  ..... heat pipe cross-sectional area
- $A_v$  ..... vapor core cross-sectional area
- $D_v$  ..... dynamic pressure coefficient for vapor flow
- $F_{x \rightarrow 1}$  .. view factor from fin to heat pipe condenser
- $F_{1 \rightarrow x}$  .. view factor from heat pipe condenser to fin
- $F_{1 \rightarrow 2}$  .. view factor from heat pipe condenser to opposit heat pipe condenser
- $F_v$  ..... frictional coefficient for vapor flow
- $h_{fg}$  ..... latent heat of vaporization
- $I$  ..... irradiation
- $k_e$  ..... effective thermal conductivity of heat pipe
- $k_f$  ..... thermal conductivity of fin
- $k_l$  ..... thermal conductivity of working fluid of heat pipe
- $k_p$  ..... thermal conductivity of heat pipe material
- $k_w$  ..... thermal conductivity of wick material of heat pipe
- $L$  ..... one half the fin length
- $M_v$  ..... mach number
- $P_v$  ..... vapor pressure
- $\Delta P_v$  .. average vapor pressure drop
- $q$  ..... heat transfer rate at heat pipe condenser segment
- $Q$  ..... heat transfer rate into single heat pipe
- $Q_c$  .... heat transfer rate by conduction
- $Q_f$  .... total heat transfer rate by conduction to the fin

$Q_{total}$  . total heat transfer rate  
 $r_o$  .... heat pipe outside radius  
 $r_i$  .... heat pipe inside radius  
 $r_v$  .... heat pipe vapor core radius  
 $R$  ..... radiosity  
 $Re_v$  . Reynolds number of vapor flow  
 $R_f$  .... reduction factor  
 $t$  ..... one half the fin thickness  
 $T$  ..... fin temperature  
 $T_E$  .... fin midpoint temperature  
 $\Delta T$  ... temperature difference  
 $T_p$  ..... heat pipe wall temperature  
 $T_{pw}$  ... temperature at the heat pipe wall-wick interface  
 $T_v$  .... vapor temperature  
 $T_{wv}$  .... temperature at the heat pipe wick-vapor interface  
 $U_{HP}$  .. overall heat transfer coefficient based on an arbitrary area  
 $U_{HP,p}$ .. overall heat transfer coefficient of heat pipe  
 $w$  ..... groove thickness  
 $w_a$  .... length of heat pipe adiabatic section  
 $w_c$  .... length of heat pipe condenser  
 $w_d$  .... groove depth  
 $w_f$  .... length of heat pipe evaporator  
 $w_f$  .... groove fin thickness

$\alpha$  ..... transmissivity of fin  
 $\beta_1$  .... radiation parameter  
 $\beta$  .....  $\epsilon_f \beta_1$   
 $\epsilon_f$  ..... emissivity of fin  
 $\epsilon_p$  ..... emissivity of heat pipe condenser  
 $\eta_f$  ..... efficiency of fin  
 $\eta_{fin}$  ... efficiency of fin and heat pipe condenser  
 $\eta_o$  ..... simple fin efficiency  
 $\mu_v$  .... vapor dynamic viscosity  
 $\rho_f$  ..... surface reflectivity of fin  
 $\rho_p$  ..... surface reflectivity of heat pipe condenser  
 $\rho_v$  ..... vapor density of heat pipe working fluid  
 $\sigma$  ..... Stephan-Boltzmann constant  
 $\theta$  ..... angular coordinate measuring position around the heat pipe condenser  
 $\theta_{min}.. \tan^{-1}[\frac{t^*}{\sqrt{r_o^2 - t^{*2}}}]$   
 $\zeta$  ..... non-dimensional distance measuring from the fin base along the fin surface

*Special symbols*

( ) ..... denote argument of function

*Superscripts*

\* ..... Non-dimensional expression

*Subscripts*

,a ..... Adiabatic section

,c ..... Condenser of heat pipe

,e ..... Evaporator of heat pipe

*Abstract*

y Performance of a grooved heat pipe radiator has been analyzed to determine its operating characteristics. A heat transfer analysis for the heat pipe is coupled with the analysis of the fin in this study. The effects of heat pipe operating temperature on heat flux and fin efficiency are investigated. Finite difference expressions are used for the grid system of the heat pipe wall and the fin.

The heat transfer coefficient of the heat pipe radiator was determined as a function of the operating temperature level. Realistic numerical results were achieved and it was shown that the required heat flux and the temperature difference between the evaporator and condenser both increase with operating temperature.

Also, the heat transfer coefficient increased with operating temperature up to a certain point, then began to level-off near a temperature of approximately 400 K. In addition, the overall efficiency of the heat pipe-fin arrangement decreased as the operating temperature level increased. JLS)

# THERMAL ANALYSIS OF HEAT PIPE RADIATORS WITH A RECTANGULAR GROOVE WICK STRUCTURE

## *I. INTRODUCTION*

### *1.1 Background*

Advanced thermal management systems are necessary for future military applications in space. The basic components of these thermal systems are heat acquisition, heat transport, and heat rejection systems. Current power levels range from 1 to 5 kW<sub>e</sub> and heat fluxes are less than 1 W/cm<sup>2</sup>. Future power levels will reach 50 - 100 kW<sub>e</sub> and heat fluxes will be approximately 100 W/cm<sup>2</sup>.

The thermal control approach employed for current spacecraft is to mount the payload on the spacecraft structure. Heat is transferred by heat conduction through the structure and then by thermal radiation from the surface of the structure to space. As power levels and thermal control requirements increase in the future, larger heat rejection area must be provided. A possible solution is to employ a heat pipe radiator. The heat pipe radiator may be designed to be fixed or deployable with two-sided heat rejection capability. The deployable radiator may also have gimbaling mechanisms to lessen radiation heat gains from the sun or albedo.

### *1.2 The Heat Pipe*

The heat pipe was developed by Grover and his associates for use in spacecraft power system[2,4], and the first analytical work was carried out by Cotter[2,4]. The heat pipe is a closed two-phase thermal device which operates without any auxiliary external pumping power. The device is basically composed of a container, a

capillary structure, and a working fluid. This simple thermal device is able to transport large quantities of heat with a very small temperature drop across the length. Furthermore, it is versatile in shape and compact in size.

The heat pipe uses phase change processes to accomplish heat transport. A conventional heat pipe is depicted in Fig.1.1. The liquid phase of the working fluid is contained in the capillary structure and the vapor phase placed in the open volume of the pipe. As heat is applied to one surface area, the so-called evaporator, the liquid in the capillary structure starts to vaporize and thus increases the vapor pressure of that section. The resulting pressure difference between the ends of the pipe causes the vapor movement carrying the latent heat of vaporization to the other end, which is called the condenser. As heat is released from the surface of the condenser, vapor is condensed in the capillary structure. This condensate returns to the evaporator by the capillary surface-tension driving force.

By choosing a suitable working fluid, the heat pipe can operate over the range of temperatures: cryogenic ( 0 - 150 K ), low temperature ( 150- 750 K ), and high temperature ( 750 - 3000 K ). The operating temperature of the heat pipe must be between the freezing and critical temperatures of the working fluid, because successful operation needs a capillary structure saturated with liquid. Heat pipes used in this study for the radiator use grooves for the capillary structure. The working fluid is water and the pipe material is copper. The useful operating temperature range of water heat pipes is from 300 K to 475 K. For this temperature range, the heat transfer through the liquid-saturated capillary structure is mainly by heat conduction and phase change takes place at the interface between the liquid and vapor. The overall temperature drop thus results mainly from the radial temperature drop through the pipe wall and capillary structure in the evaporator and condenser section.

### *1.3 Objectives of the Study*

The primary purpose of this study has been to analytically investigate normal operating characteristics of a water heat pipe radiator and the thermal efficiency of radiator fins as a function of the radiation parameter. For this purpose, a mathematical model and a numerical solution technique has been developed.

Given the operating heat pipe temperature and the applied heat to the evaporator, temperatures such as the surface temperatures of the evaporator and condenser and the interface temperatures between the liquid and vapor at these sections have been determined. The overall heat transfer coefficient has also been found as functions of the operating temperature and heat input.

Using the results from the heat pipe analysis, the thermal efficiency of the radiator fins has been investigated. For this analysis, it is assumed that the radiator surface is a gray body, which has the same value for the emissivity and absorptivity.

### *1.4 Literature Survey*

Before discussing the details of this thesis, a review of the literature relating to fin-radiator studies is appropriate.

Lieblin(1959) studied the heat transfer characteristics of a radiator with rectangular fins. It was assumed that the fin had a uniform temperature at the edge, and no consideration was given to the effects of fin-tube mutual irradiation.

Sparrow, Eckert, and Irvine(1961) studied the general case of a radiator with longitudinal or annular fins, which included mutual irradiation effects between the fin and tube, which was reflected in their governing heat transfer relations.

Annular circular fins with a black surface attached to the circular tubes was also analyzed by Sparrow(1962) with consideration of mutual irradiation effects.

Sparrow and Eckert(1962) studied the effects of mutual irradiation occurring between a fin and a base surface with black surfaces. They found that the fin heat



loss was significantly reduced by the presence of the base surfaces in the range of practical operating conditions. Additionally, the base heat surface heat loss comprised an important part of the total heat loss from the given system. They also formulated the equation for the selective gray surfaces and arbitrary irradiation from external sources, and analyzed circular black tubes with longitudinal fins of negligible thickness.

Sarabia and Hitchcock(1966) formulated the heat transfer equations for fin-tube radiators with gray, diffuse emitting and absorbing surfaces. A numerical method was also developed and the accuracy of the correlation between the gray and black surface was established.

The total weight of an energy conversion system is very important for space applications. The temperature level of the radiator influences the total weight required to dissipate the radiation into space. For design studies utilizing finned-tube radiators, the results of references 14 and 3 can be used to determine approximately the optimum operating radiator temperature and optimum tube radius to fin length ratio.

Rolf-Dieter and Walter(1962) studied the minimum configurations of tube-fin radiators with gray surfaces and the governing by non-linear integro-differential equation which can be solved by successive approximations using Galerkin's method.

From the literature search, it is evident that there is considerable interest in the high thermal heat transfer radiator for space applications. Here, the study of the characteristics of the heat pipe-fin radiator, which may be used for space applications, has been carried out numerically.

## II. MATHEMATICAL ANALYSIS

Figure 2.1 depicts a grooved schematic of the heat pipe radiator for space applications. Its cross-sectional view is shown in Fig.2.2, which presents grooved heat pipes connected by rectangular fins. This chapter describes a mathematical analysis under the following assumptions:

- (a) Heat transfer from the heat pipe condenser surface is by radiation only.
- (b) Heat fluxes into the evaporator and the condenser are uniform.
- (c) Heat pipe condenser has a constant temperature distribution along the heat pipe axis.
- (d) Heat flow in the heat pipe is one dimensional.
- (e) Vapor flow in the heat pipe is laminar and incompressible.
- (f) Temperature of the fin base is constant along the length of the heat pipe condenser.
- (g) Heat pipe radiator is exposed to deep space.

### 2.1 Heat Balance Equation

**2.1.1 Heat Pipe Section** The primary heat transfer mechanisms for the low-temperature heat pipe are (i) heat conduction across the container wall and the liquid-saturated wick at the evaporator section, (ii) convective transport of latent heat by vapor from the evaporator to the condenser, and (iii) heat conduction across the liquid-saturated wick and the container wall at the condenser section. The heat conduction in the pipe wall and in the liquid-saturated wick can be described by *Fourier's Law* as follows :

$$Q = \frac{\Delta T}{R}$$

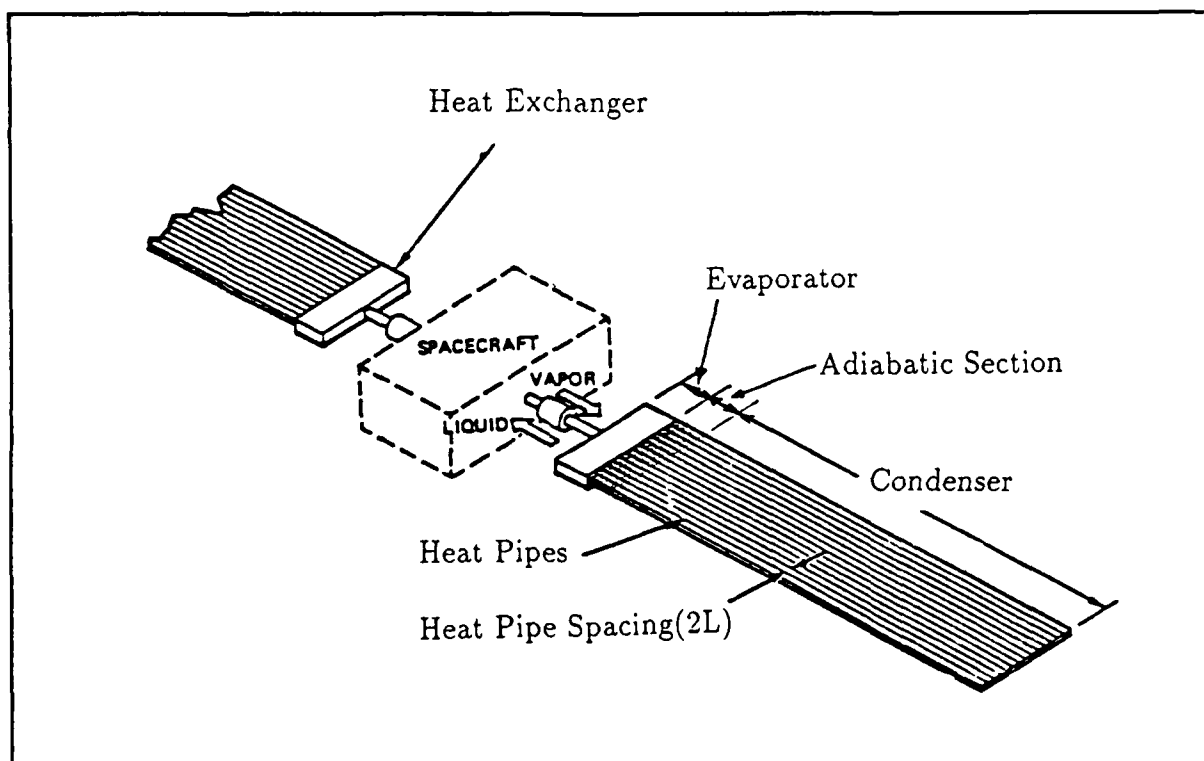


Figure 2.1. Multiple Heat Pipe Radiator in the Spacecraft

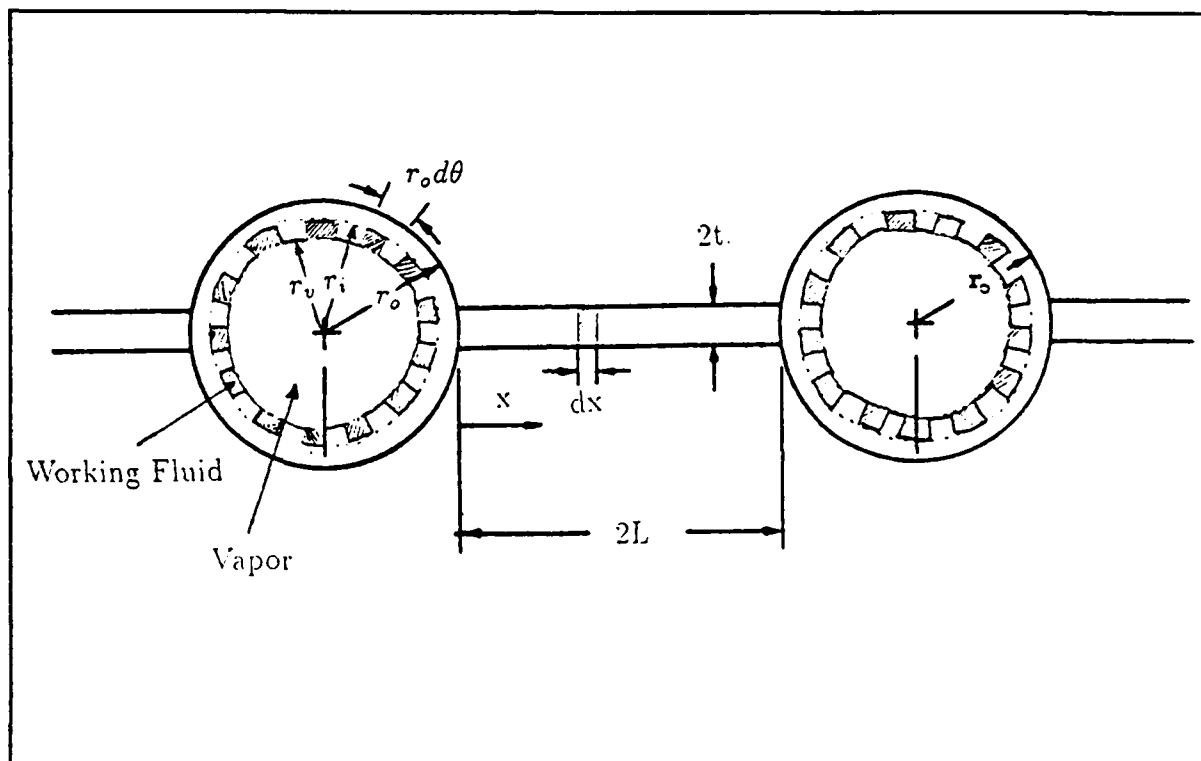


Figure 2.2. The Cross-Sectional View of the Condenser Section of Heat Pipe Radiator

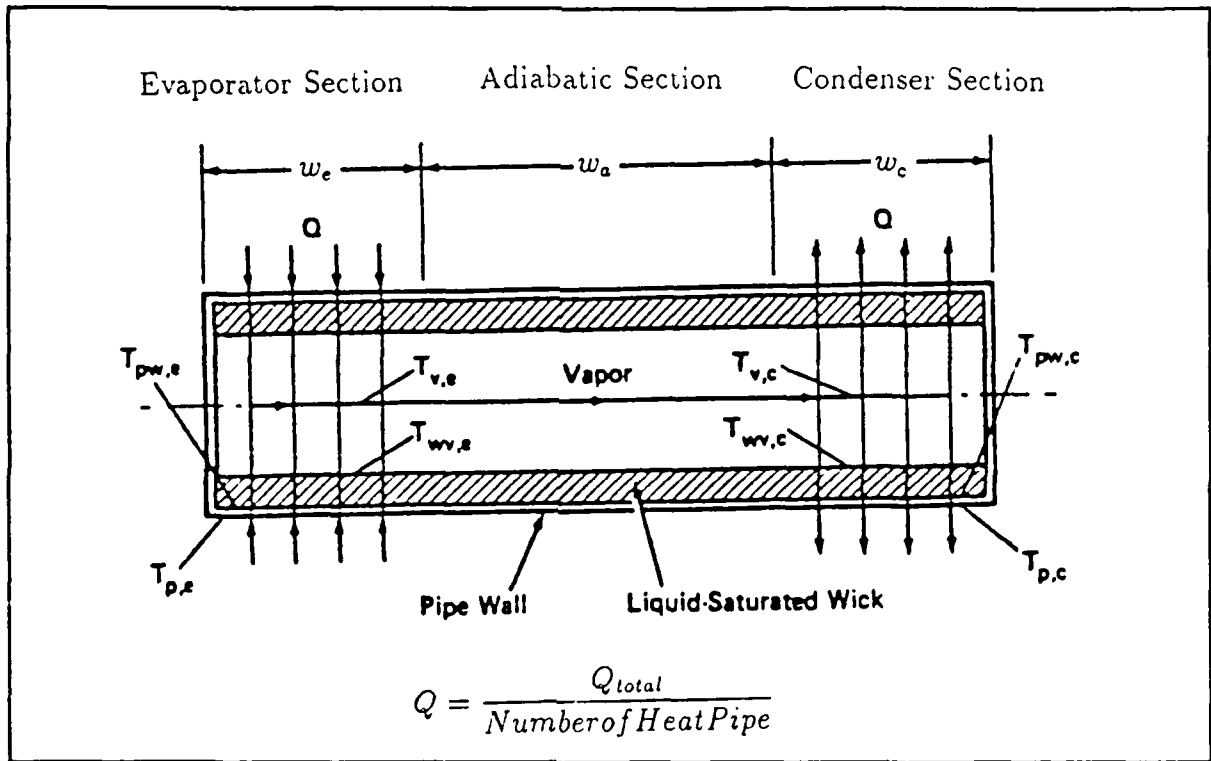


Figure 2.3. Sketch of Heat Flow Path through a Single Heat Pipe

where  $\Delta T$  is the temperature drop through the wall and  $R$  is the thermal resistance, which can be evaluated from expressions for the cylinder wall:

$$R = \frac{\ln(r_2/r_1)}{2\pi \cdot w \cdot k}$$

where  $k$  is the thermal conductivity of the heat pipe wall material and  $w$  is the length of heat pipe wall. The axial heat convection by vapor can be described by the *Clausius-Clapeyron equation* which relates the vapor temperature and pressure as follows :

$$T_1 - T_2 = \frac{T_v(P_1 - P_2)}{\rho_v \cdot h_{fg}}$$

where  $h_{fg}$  is the latent heat of the vaporization,  $T_v$  is the vapor temperature of working fluid, and  $\rho_v$  is the vapor density of working fluid.

Application of the above equations to each section in a series of heat flow paths in a conventional heat pipe as shown in Fig. 2.3, with the temperatures at the different locations indicated, yields

- Pipe Wall at Evaporator :

$$T_{p,e} - T_{pw,e} = \frac{\ln(r_o/r_i)}{2\pi \cdot w_e \cdot k_p} Q \quad (2.1)$$

where  $k_p$  is the thermal conductivity of the heat pipe container, and  $w_e$  is the length of the heat pipe evaporator.

- Liquid-Saturated Wick at Evaporator :

$$T_{pw,e} - T_{wv,e} = \frac{\ln(r_i/r_v)}{2\pi \cdot w_e \cdot k_{e,e}} Q \quad (2.2)$$

where  $k_{e,e}$  is the effective thermal conductivity of the evaporator capillary structure ( See Table 2.1).

- Axial Vapor Passage :

$$T_{v,e} - T_{v,c} = \frac{T_v(P_{v,e} - P_{v,c})}{\rho_v \cdot h_{fg} \cdot Q} Q \quad (2.3)$$

- Liquid-Saturated Wick at Condenser :

$$T_{wv,c} - T_{pw,c} = \frac{\ln(r_i/r_v)}{2\pi \cdot w_c \cdot k_{e,c}} Q \quad (2.4)$$

where  $k_{e,c}$  is the effective thermal conductivity of the condenser capillary structure ( See Table 2.1 ).

- Pipe Wall at Condenser :

$$T_{pw,c} - T_{p,c} = \frac{\ln(r_o/r_i)}{2\pi \cdot w_c \cdot k_p} Q \quad (2.5)$$

Table 2.1. Expressions of Effective Thermal Conductivity  $k_e$  for Liquid-Saturated Wicks

Rectangular grooves	$k_e$ Expressions
Evaporator	$k_{e,e} = \frac{(w_f w_d k_l k_w) + w k_l (0.185 w_f k_w + w_d k_l)}{(w_f + w)(0.185 w_f k_w + w_d k_l)}$
Condenser	$k_{e,c} = \frac{w k_l + w_f k_w}{w + w_f}$
<p>Where <math>k_l</math> = liquid thermal conductivity  <math>k_w</math> = thermal conductivity of wick material  <math>w</math> = groove thickness  <math>w_f</math> = groove fin thickness  <math>w_d</math> = groove depth</p>	

Combining all these equations, Eqs.(2.1)-(2.5), results in

$$T_{p,e} - T_{p,c} = Q \left[ \frac{\ln(r_o/r_i)}{2\pi \cdot w_e \cdot k_p} + \frac{\ln(r_i/r_v)}{2\pi \cdot w_e \cdot k_{e,e}} + \frac{T_v(P_{v,e} - P_{v,c})}{\rho_v \cdot h_{fg} \cdot Q} + \frac{\ln(r_i/r_v)}{2\pi \cdot w_c \cdot k_{e,c}} + \frac{\ln(r_o/r_i)}{2\pi \cdot w_c \cdot k_p} \right] \quad (2.6)$$

The total heat transfer of the heat pipe is defined as

$$Q = AU_{HP}(T_{p,e} - T_{p,c}) \quad (2.7)$$

where  $T_{p,e}$  is the outer surface temperature of the evaporator,  $T_{p,c}$  is the outer surface temperature of the condenser, and  $U_{HP}$  is the overall heat transfer coefficient based

on an arbitrary area,  $A$ . Note that  $A$  may be the cross-sectional area of the pipe  $A_p$ , the surface area of the evaporator  $A_e$ , the surface area of the condenser  $A_c$ , or any other area. By nature of the definition for  $U_{HP}$ , it follows that

$$AU_{HP} = A_p U_{HP,p} = A_e U_{HP,e} = A_c U_{HP,c}$$

Choosing the cross-sectional area for this area, Eq.(2.7) becomes

$$Q = A_p U_{HP,p} (T_{p,e} - T_{p,c}) \quad (2.8)$$

where  $A_p$  is  $\pi r_o^2$ . Therefore, from Eqs.(2.7) and (2.8),

$$U_{HP,p} = \left[ \frac{r_o^2}{2w_e \cdot k_p} \ln\left(\frac{r_o}{r_i}\right) + \frac{r_o^2}{2w_e \cdot k_{e,e}} \ln\left(\frac{r_i}{r_v}\right) + \frac{\pi r_o^2 T_v (P_{v,e} - P_{v,c})}{\rho_v \cdot h_{fg} \cdot Q} \right. \\ \left. + \frac{r_o^2}{2w_c \cdot k_{e,c}} \ln\left(\frac{r_i}{r_v}\right) + \frac{r_o^2}{2w_c \cdot k_p} \ln\left(\frac{r_o}{r_i}\right) \right]^{-1} \quad (2.9)$$

The vapor pressure drop,  $P_{v,e} - P_{v,c}$  in Eq.(2.9), is the sum of the average vapor pressure drops in the evaporator, the adiabatic section, and the condenser.

$$P_{v,e} - P_{v,c} = \Delta \bar{P}_{v,e} + \Delta \bar{P}_{v,a} + \Delta \bar{P}_{v,c} \quad (2.10)$$

These components of the vapor pressure drop can be obtained by integrating the following equation which is derived from the axial momentum flux law [1],

$$\frac{dP_v}{dx} = -F_v Q - D_v \frac{dQ^2}{dx} \quad (2.11)$$

Here,  $F_v$  and  $D_v$  are respectively the frictional and the dynamic pressure coefficients for the vapor flow, which are dependent upon flow conditions( see Table 2.2).

When the vapor flow is assumed to be laminar and incompressible with negligible dynamic effect and the distribution of heat flux as along the evaporator and



Table 2.2. Expressions of Vapor Frictional Coefficient  $F_v$  and Dynamic Coefficient  $D_v$

For circular vapor core cross section		
Flow conditions	$F_v$	$D_v$
$Re_v < 2300$ $M_v < 0.2$	$\frac{8\mu_v}{r_v^2 A_v \rho_v h_{fg}}$	$\frac{1.33}{A_v^2 \rho_v h_{fg}^2}$
$Re_v < 2300$ $M_v > 0.2$	$(\frac{8\mu_v}{r_v^2 A_v \rho_v h_{fg}})(1 + \frac{\gamma_v - 1}{2} M_v^2)^{-1/2}$	$\frac{1.33}{A_v^2 \rho_v h_{fg}^2}$
$Re_v > 2300$ $M_v < 0.2$	$(\frac{0.019\mu_v}{A_v r_v \rho_v h_{fg}})(\frac{2r_v Q}{A_v h_{fg} \mu_v})^{3/4}$	$\frac{1}{A_v^2 \rho_v h_{fg}^2}$
$Re_v > 2300$ $M_v > 0.2$	$(\frac{0.019\mu_v}{A_v r_v^2 \rho_v h_{fg}})(\frac{2r_v Q}{A_v h_{fg} \mu_v})^{3/4}(1 + \frac{\gamma_v - 1}{2} M_v^2)^{-3/4}$	$\frac{1}{A_v^2 \rho_v h_{fg}^2}$
$Re_v$ = Reynolds number of vapor flow $M_v$ = Mach number $A_v$ = Vapor flow area( $\pi r_v^2$ ) $\mu_v$ = Viscosity of vapor		

condenser uniform, the average pressure drop through each section can be expressed as follows:

$$\Delta \bar{P}_{v,e} = \frac{F_v w_e Q}{6}$$

$$\Delta \bar{P}_{v,a} = F_v w_a Q$$

$$\Delta \bar{P}_{v,c} = \frac{F_v w_c Q}{6}$$

Therefore,

$$P_{v,e} - P_{v,c} = F_v Q \left( \frac{w_e}{6} + w_a + \frac{w_c}{6} \right) \quad (2.12)$$

Substituting Eq.(2.12) into Eq.(2.6) gives

$$\begin{aligned} T_{p,c} = T_{p,e} - Q \left[ \frac{\ln(r_o/r_i)}{2\pi \cdot w_e \cdot k_p} + \frac{\ln(r_i/r_v)}{2\pi \cdot w_e \cdot k_{e,e}} + \frac{T_v F_v (w_e/6 + w_a + w_c/6)}{\rho_v \cdot h_{fg}} \right. \\ \left. + \frac{\ln(r_i/r_v)}{2\pi \cdot w_c \cdot k_{e,c}} + \frac{\ln(r_o/r_i)}{2\pi \cdot w_c \cdot k_p} \right] \end{aligned} \quad (2.13)$$

### 2.1.2 Heat Pipe Condenser Section with Fin

**2.1.2.1 Fin Surface** The basic thermal analysis of the heat pipe condenser analysis with an extended fin surface is the conservation of energy law. The terminology and coordinate system for the longitudinal fin of rectangular profile radiating to deep space are shown in Fig. 2.4. This figure also shows the assumed direction of heat flow for a typical fin segment. For this fin segment, symmetrical heat transfer from both (i.e., upper and lower) surfaces of the fin is assumed. Under steady-state conditions, energy conservation for the differential fin element  $dx$  takes the form of a balance between net conduction and net radiation effects.

$$(dQ_{cond})_{net} + (dQ_{rad})_{net} = 0 \quad (2.14)$$

The fin receives heat on its faces from both heat pipe condenser tubes. Heat enters into the fin uniformly at its base where  $x = 0$ . Referring to Fig.2.4, the heat balance

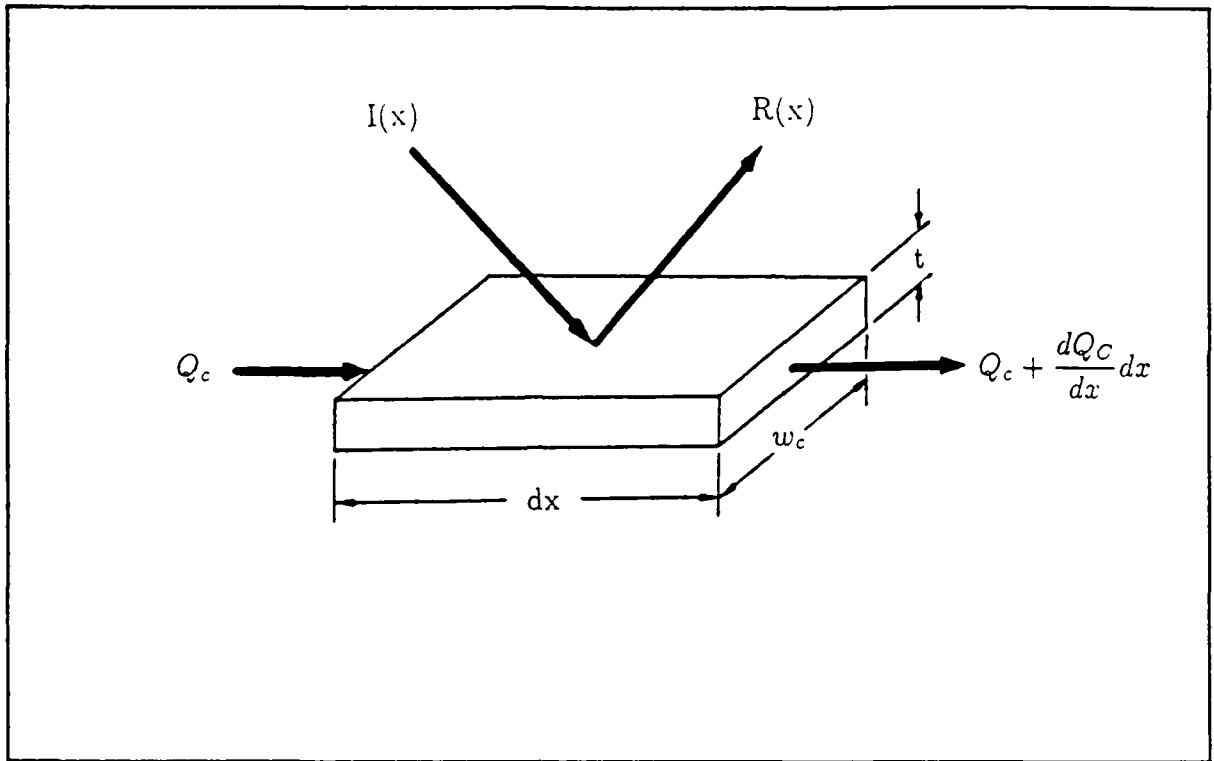


Figure 2.4. Heat Flow Path in a Differential Fin Element

equation for the differential element  $dx$  is

$$Q_c + I(x)w_c dx = Q_c + \frac{dQ_c}{dx}dx + R(x)w_c dx \quad (2.15)$$

*Fourier's law* for one-dimensional heat conduction gives

$$\frac{dQ_c}{dx} = -k_f \cdot w_c \cdot t \frac{d^2 T}{dx^2} \quad (2.16)$$

where  $k_f$  is the conductivity of the fin, which is made from the same material as the heat pipe, and  $w_c$  is the length of heat pipe condenser. Combining Eqs.(2.15) and (2.16) yields

$$I(x)w_c dx = [-k_f \cdot w_c \cdot t \frac{d^2 T}{dx^2}]dx + R(x)w_c dx$$

or

$$k_f \cdot t \frac{d^2 T}{dx^2} = R(x) - I(x)$$

Thus,

$$\frac{d^2 T}{dx^2} = \frac{1}{k_f \cdot t} [R(x) - I(x)] \quad (2.17)$$

Eq.(2.17) may be placed in a dimensionless form by introducing a dimensionless temperature,  $T^* = T/T_{p,c}$ , and a dimensionless position variable,  $\zeta = x/L$  :

$$\frac{d^2 T^*}{d\zeta^2} = \beta_1 [R^*(\zeta) - I^*(\zeta)] \quad (2.18)$$

where

$$R^*(\zeta) = \frac{R(x)}{\sigma T_{p,c}^4} \quad I^*(\zeta) = \frac{I(x)}{\sigma T_{p,c}^4}$$

and

$$\beta_1 = \frac{\sigma T_{p,c}^3 \cdot L^2}{k_f \cdot t} \quad (2.19)$$

The radiosity of the fin element,  $R(x)$ , consists of the emission from the surface of the fin element plus the reflected irradiation from both condenser base surfaces.

$$R(x)w_c dx = \epsilon_f(\sigma T^4 w_c dx) + \rho_f(I(x)w_c dx) \quad (2.20)$$

In dimensionless form, Eq.(2.20) becomes

$$R^*(\zeta) = \epsilon_f T^{*4} + [1 - \epsilon_f] I^*(\zeta) \quad (2.21)$$

where  $\rho_f = 1 - \epsilon_f$ , since the transmissivity,  $\tau_f$ , is zero for the opaque fin surface, and  $\alpha_f = \epsilon_f$  for black or gray body surfaces. Substituting Eq.(2.21) into (2.18) yields

$$\frac{d^2 T^*}{d\zeta^2} = \beta T^{*4} - \beta I^*(\zeta) \quad (2.22)$$

where

$$\beta = \beta_1 \cdot \epsilon_f = \frac{\sigma T_{p,c}^3 L^2 \epsilon_f}{k_f \cdot t}$$

The boundary conditions are for the governing equation as follows:

at  $\zeta = 1$ ,

$$T^* = T_E^* \quad \frac{dT^*}{d\zeta} = 0 \quad (2.23)$$

at  $\zeta = 0$ ,

$$T^* = 1 \quad (2.24)$$

Integrating Eq.(2.22) once gives

$$\frac{dT^*}{d\zeta} = -A[T^{*5} - T_E^{*5}] + 5[I_t^* - \int_0^\zeta I^*(\zeta) \frac{dT^*}{d\zeta} d\zeta]^{1/2} \quad (2.25)$$

where

$$A = 0.6325\sqrt{\beta}$$

and

$$I_t^* = \int_0^1 I^*(\zeta) \left[ \frac{dT^*}{d\zeta} \right] d\zeta$$

Finally, the temperature at the new axial position is approximated by using the Taylor series expansion,

$$T^*(\zeta + \Delta\zeta) = T^*(\zeta) + \frac{dT^*}{d\zeta} \Big|_\zeta \Delta\zeta + \frac{1}{2} \frac{d^2 T^*}{d\zeta^2} \Big|_\zeta (\Delta\zeta)^2 \quad (2.26)$$

where the derivatives are obtained from Eqs.(2.25) and (2.22).

The irradiation of the fin element surface,  $I(x)$ , consists of the radiosity received from both heat pipe condensers, i.e., heat pipe condenser 1 and condenser 2. It can

be expressed as

$$I(x)w_c dx = \int_{\theta_1} R(\theta_2)F_{1 \rightarrow x} w_c r_o d\theta_1 + \int_{\theta_2} R(\theta_2)F_{2 \rightarrow x} w_c r_o d\theta_2 \quad (2.27)$$

In dimensionless form, Eq.(2.27) becomes

$$I^*(\zeta)d\zeta = \int_{\theta_1} R^*(\theta_1)F_{1 \rightarrow \zeta} r_o^* d\theta_1 + \int_{\theta_2} R^*(\theta_2)F_{2 \rightarrow \zeta} r_o^* d\theta_2 \quad (2.28)$$

where

$$r_o^* = \frac{r_o}{L}$$

**2.1.2.2 Condenser Base Surface** Assuming the temperature of the condenser surface is uniform, an expression for heat loss can now be derived. Considering the condenser surface 1 ( Fig.2.2 ), the net heat loss is expressed as the difference between the radiant emission and the incoming energy radiated from the fin and the condenser surface 2. Therefore the heat balance equation for the condenser surface element ( $w_c r_o d\theta$ ) becomes

$$q(\theta)w_c r_o d\theta + I(\theta)w_c r_o d\theta = R(\theta)w_c r_o d\theta \quad (2.29)$$

In dimensionless form, Eq.(2.29) becomes

$$q^*(\theta) = R^*(\theta) - I^*(\theta) \quad (2.30)$$

where

$$q^*(\theta) = \frac{q(\theta)}{\sigma T_{p,c}^4}$$

$$R^*(\theta) = \frac{R(\theta)}{\sigma T_{p,c}^4}$$

and

$$I^*(\theta) = \frac{I(\theta)}{\sigma T_{p,c}^4}$$

The radiosity of condenser base surface,  $R(\theta)$ , consists of the condenser base surface emission plus the reflected irradiation and can be expressed as

$$R(\theta)w_c r_o d\theta = \epsilon_p[(\sigma T_{p,c}^4)w_c r_o d\theta] + \rho_p[I(\theta)w_c r_o d\theta] \quad (2.31)$$

In dimensionless form, Eq.(2.31) becomes

$$R^*(\theta) = \epsilon_p + (1 - \epsilon_p)I^*(\theta) \quad (2.32)$$

where

$$\rho_p = 1 - \epsilon_p$$

Substituting Eq.(2.32) into Eq.(2.30) yields

$$q^*(\theta) = \epsilon_p[1 - I^*(\theta)] \quad (2.33)$$

The irradiation of condenser surface 1,  $I(\theta_1)$ , consists of the radiosity received from the fin and the condenser surface 2.

$$I(\theta_1)w_c r_o d\theta_1 = \int_x R(x)F_{x \rightarrow 1}w_c dx + \int_{\theta_2} R(\theta_2)F_{2 \rightarrow 1}w_c r_o d\theta_2 \quad (2.34)$$

From the reciprocity relationship

$$F_{x \rightarrow 1}w_c dx = F_{1 \rightarrow x}w_c r_o d\theta_1 \quad (2.35)$$

Substituting Eq.(2.35) into Eq.(2.34) yields

$$I(\theta_1)w_c r_o d\theta_1 = \int_x R(x)F_{1 \rightarrow x}w_c r_o d\theta_1 + \int_{\theta_2} R(\theta_2)F_{2 \rightarrow 1}w_c r_o d\theta_2 \quad (2.36)$$

In dimensionless form, Eq.(2.36) becomes

$$I^*(\theta_1)d\theta_1 = \int_{\zeta} R^*(x)F_{1 \rightarrow \zeta}d\theta_1 + \int_{\theta_2} R^*(\theta_2)F_{2 \rightarrow 1}d\theta_2 \quad (2.37)$$

where

$$R^*(x) = \frac{R(x)}{\sigma T_{p,c}^4}$$

## 2.2 Heat Transfer

**2.2.1 Fin Surface** The fin heat transfer rate can be expressed by

$$Q_f = -k_f \cdot w_c \cdot t \frac{dT}{dx} \Big|_{x=0} \quad (2.38)$$

The fin efficiency,  $\eta_{fin}$ , is defined as the ratio of the heat transferred by the fin to the heat that could be dissipated by an isothermal black fin of the same dimensions, and can be expressed as follows:

$$\eta_{fin} = \frac{Q_f}{\sigma T_{p,c}^4 w_c L}$$

from Eq.(2.38)

$$\eta_{fin} = -\frac{k_f \cdot w_c \cdot t}{\sigma T_{p,c}^4 \cdot w_c \cdot L} \frac{dT}{dx} \Big|_{x=0}$$

$$\eta_{fin} = -\frac{1}{\beta_1} \frac{dT^*}{d\zeta} \Big|_{\zeta=0} \quad (2.39)$$

where

$$\zeta = \frac{x}{L}, \quad \text{and} \quad \beta_1 = \frac{\sigma T_{p,c}^3 L^2}{k_f t}$$

**2.2.2 Total Surface** The total heat transfer rate can be expressed by

$$Q_{total} = 4 \left[ \int_{\theta} q(\theta) w_c r_o d\theta + Q_f \right] \quad (2.40)$$



The overall fin-condenser efficiency,  $\eta_{eff}$ , is defined as the ratio of the heat transferred from the heat pipe condenser and the fin to the heat that could be dissipated by a flat, black surface of the same total length as the heat pipe condenser and the fin. Therefore,

$$\eta_{eff} = \frac{Q_{total}}{4[\sigma T_{p,c}^4(L + \sqrt{r_o^2 - t^2})w_c]} \quad (2.41)$$

Combining Eqs.(2.40) and (2.41) gives

$$\eta_{eff} = \frac{\int_{\theta} (q(\theta)w_c r_o) d\theta + Q_f}{\sigma T_{p,c}^4 w_c [L + \sqrt{r_o^2 - t^2}]}$$

or

$$\eta_{eff} = \frac{r_o^*}{B} \int_{\theta_{min}}^{\frac{\pi}{2}} q^*(d\theta) + \frac{\eta_{fin}}{B} \quad (2.42)$$

where

$$B = 1 + \sqrt{r_o^{*2} - t^{*2}}$$

Substituting Eq.(2.33) into Eq.(2.42) yields

$$\eta_{eff} = \frac{r_o^*}{B} \int_{\theta_{min}}^{\frac{\pi}{2}} \epsilon_p [1 - I^*(\theta)] d\theta + \frac{\eta_{fin}}{B}$$

or

$$\eta_{eff} = C_t \left[ \frac{\pi}{2} - \theta_{min} - D_t \right] + \frac{\eta_{fin}}{B} \quad (2.43)$$

where

$$C_t = \frac{r_o^* \epsilon_p}{1 + \sqrt{r_o^{*2} - t^{*2}}}, \quad \theta_{min} = \tan^{-1} \left[ \frac{t^*}{\sqrt{r_o^{*2} - t^{*2}}} \right]$$

and

$$D_t = \int_{\theta_{min}}^{\frac{\pi}{2}} I^*(\theta) d\theta$$

### III. COMPUTATIONAL PROCEDURE

#### 3.1 Summary of Equations and Finite Difference Forms

Eq.(2.12) :

$$P_{v,e} - P_{v,c} = F_v Q \left( \frac{w_e}{6} + w_a = \frac{w_c}{6} \right)$$

Eq.(2.3) :

$$T_{v,e} - T_{v,c} = \frac{T_v(P_{v,e} - P_{v,c})}{\rho_v \cdot h_{fg} \cdot Q} Q$$

Eq.(2.2) :

$$T_{pw,e} = T_{wv,e} + \frac{\ln(r_i/r_v)}{2\pi \cdot w_e \cdot k_{e,e}} Q$$

Eq.(2.1) :

$$T_{p,e} = T_{pw,e} + \frac{\ln(r_o/r_i)}{2\pi \cdot w_e \cdot k_p} Q$$

Eq.(2.4) :

$$T_{pw,c} = T_{wv,c} - \frac{\ln(r_i/r_v)}{2\pi \cdot w_c \cdot k_{e,c}} Q$$

Eq.(2.5) :

$$T_{p,c} = T_{pw,c} - \frac{\ln(r_o/r_i)}{2\pi \cdot w_c \cdot k_p} Q$$

Eq.(2.6) :

$$T_{p,e} - T_{p,c} = Q \left[ \frac{\ln(r_o/r_i)}{2\pi \cdot w_e \cdot k_p} + \frac{\ln(r_i/r_v)}{2\pi \cdot w_e \cdot k_{e,e}} \right. \\ \left. + \frac{T_v(P_{v,e} - P_{v,c})}{\rho_v \cdot h_{fg} \cdot Q} + \frac{\ln(r_i/r_v)}{2\pi \cdot w_c \cdot k_{e,c}} + \frac{\ln(r_o/r_i)}{2\pi \cdot w_c \cdot k_p} \right]$$

Eq.(2.9) :

$$U_{HP,p} = \left[ \frac{r_o^2}{2w_e \cdot k_p} \ln(r_o/r_i) + \frac{r_o^2}{2w_e \cdot k_{e,e}} \ln(r_i/r_v) + \frac{\pi r_o^2 T_v(P_{v,e} - P_{v,c})}{\rho_v \cdot h_{fg} \cdot Q} \right]$$

$$+ \frac{r_o^2}{2w_c \cdot k_{e,c}} \ln(r_i/r_v) + \frac{r_o^2}{2w_c \cdot k_p} \ln(r_o/r_i)]_{-1}$$

From Eq.(2.19)

$$\beta_1 = \frac{\sigma T_{p,c}^3 L^2}{k_f \cdot t}$$

Eq.(2.27) :

$$I^*(\zeta) d\zeta = \int_{\theta_1} R^*(\theta_1) F_{1 \rightarrow x} r_o^* d\theta_1 + \int_{\theta_2} R^*(\theta_2) F_{2 \rightarrow x} r_o^* d\theta_2$$

In a finite difference form , this becomes

$$I^*(\zeta) = \sum_{\theta_{min}}^{\pi/2} R^*(\theta_1) F_{1 \rightarrow x} A_{r1} + \sum_{\theta_{min}}^{\pi/2} R^*(\theta_2) F_{2 \rightarrow x} A_{r2} \quad (3.1)$$

where

$$A_{r1} = r_o^* \frac{\Delta\theta_1}{\Delta\zeta}, \quad A_{r2} = r_o^* \frac{\Delta\theta_2}{\Delta\zeta}$$

and

$$\theta_{min} = \tan^{-1} \left( \frac{t^*}{\sqrt{r_o^{*2} - t^{*2}}} \right)$$

Eq.(2.21) :

$$\frac{d^2 T^*}{d\zeta^2} = \beta T^{*4} - \beta I^*(\zeta)$$

Eq.(2.24) : reduces into a finite difference equation as

$$\frac{dT^*}{d\zeta} = -A \{ \{T^{*5} - T_E^{*5}\} + 5 \{ I_t^* - \sum_0^{\zeta} I^*(\zeta) \frac{dT^*}{d\zeta} \Delta\zeta \} \}^{1/2} \quad (3.2)$$

where

$$A = 0.6325 \sqrt{\beta}$$

$$I_t^* = \sum_0^1 I^*(\zeta) \left[ \frac{dT^*}{d\zeta} \right] \Delta\zeta$$

and

$$\beta = \frac{\sigma T_{p,c}^3 L^2 \epsilon_f}{k_f t}$$

Eq.(2.25) :

$$T^*(\zeta + \Delta\zeta) = T^*(\zeta) + \frac{dT^*}{d\zeta}|_{\zeta}\Delta\zeta + \frac{1}{2} \frac{d^2T^*}{d\zeta^2}|_{\zeta}(\Delta\zeta)^2$$

Eq.(2.20) :

$$R^*(\zeta) = \epsilon_f T^{*4} + [1 - \epsilon_f] I^*(\zeta)$$

Eq.(2.36)

$$I^*(\theta_1) d\theta_1 = \int_{\theta_1} R^*(\zeta) F_{1 \rightarrow \zeta} d\theta_1 + \int_{\theta_2} R^*(\theta_2) F_{2 \rightarrow 1} d\theta_2$$

Converting into the finite difference equation,

$$I^*(\theta_1) = \sum_0^1 R^*(\zeta) F_{1 \rightarrow \zeta} + \sum_{\theta_{min}}^{\pi/2} R^*(\theta_2) F_{2 \rightarrow 1} \frac{\Delta\theta_2}{\Delta\theta_1} \quad (3.3)$$

Eq.(2.31) :

$$R^*(\theta) = \epsilon_p + (1 - \epsilon_p) I^*(\theta)$$

From Eq.(2.42)

$$\eta_{eff} = C_t \left[ \frac{\pi}{2} - \theta_{min} - \sum_{\theta_{min}}^{\pi/2} I^*(\theta) \Delta\theta \right] + \frac{\eta_{fin}}{B} \quad (3.4)$$

where

$$C_t = \frac{r_o^* \epsilon_p}{B}$$

and

$$B = 1 + \sqrt{r_o^{*2} - t^{*2}}$$

### 3.2 Initial Values

Because of symmetry, the midpoint of the fin is considered to be adiabatic. Therefore, the energy balance for this differential control volume is

$$\epsilon_f \sigma T_E^4 w_c dx = 2 \int_{\theta_{min}}^{\frac{\pi}{2}} R(\theta) F_{1 \rightarrow E} w_c r_o d\theta \quad (3.5)$$

or, in dimesionless form,

$$T_E^{*4} d\zeta = 2r_o^* \int_{\theta_{min}}^{\frac{\pi}{2}} R^*(\theta) F_{1 \rightarrow E} d\theta \quad (3.6)$$

The initial condenser surface radiation is assumed to be equal to the condenser surface emission :

$$R(\theta) w_c r_o d\theta = \epsilon_p \sigma T_{p,c}^4 w_c r_o d\theta \quad (3.7)$$

In dimensionless form, Eq.(2.21) becomes

$$R^*(\theta) = \epsilon_p \quad (3.8)$$

Substituting Eq.(2.24) into Eq.(3.1) yields

$$T_E^{*4} d\zeta = 2r_o^* \epsilon_p \int_{\theta_{min}}^{\pi/2} F_{1 \rightarrow E} d\theta \quad (3.9)$$

Expressing Eq.(3.9) in finite difference form yields

$$T_E^{*4} = 2r_o^* \epsilon_p \sum_{\theta_{min}}^{\pi/2} F_{1 \rightarrow E} \frac{\Delta \theta}{\Delta \zeta} \quad (3.10)$$

or

$$T_E^* = 1.189 [\epsilon_p r_o^* \frac{\Delta \theta}{\Delta \zeta} \sum_{\theta_{min}}^{\frac{\pi}{2}} F_{1 \rightarrow E}]^{1/4} \quad (3.11)$$

Even if the irradiation on the fin midpoint, as expressed in Eq.(3.3), is small, the lowest value that the fin midpoint temperature can have must still be larger than that for the case of fins with no irradiation. The solution to the simple fin problem is included in Appendix D. A fifth order polynomial expression for the simple fin edge temperature( fin midpoint ) as a function of the radiation parameter,  $\beta$ , is given in Eq.(D.3), Appendix D.

The initial midpoint temperature assumed in this solution was the one calculated by Eq.(3.3) or Eq.(D.3), whichever was greater. The initial temperature gradient along the fin was computed with the following equations :

$$\frac{dT^*}{d\zeta}|_i = -A[T^{*5} - T_E^{*5}]^{1/2} \quad (3.12)$$

and

$$T^*(\zeta + \Delta\zeta)|_i = T^*(\zeta) + \frac{dT^*}{d\zeta}|_i d\zeta \quad (3.13)$$

Equation(3.2) shows that the temperature gradient depends on the value of  $I_i$  which in turn depends on the product of the irradiation and the temperature gradient. The initial values of the temperature gradient, Eq.(3.12), are too large near the fin base. Therefore, in order to attenuate this initial error, the following linear reduction factor,  $R_f$ , was used for the first 10 iterations and applied to the fin irradiation :

$$I^*(\zeta) = I^*(\zeta)R_f \quad (3.14)$$

where

$$R_f = \frac{n}{10} \quad \text{for } n < 10$$

$$R_f = 1.0 \quad \text{for } n > 10$$

In order to preclude obtaining results that include the reduction factor, the criteria for ending a solution included the requirement that at least 15 iterations be performed in all cases.

### 3.3 Method of Calculation

*Step 1 :* Choose an appropriate operating temperature level.

*Step 2 :* Assume  $T_{p,c}$  is approximately the same as the given operating temperature.

*Step 3 :* As a first guess, estimate the required heat input using Eq. (2.41).

*Step 4 :* Solve Eq. (2.12) to determine the vapor pressure drop.

*Step 5 :* Solve Eq. (2.3) to determine the temperature difference between evaporator and condenser surfaces.

*Step 6 :* Solve Eqs. (2.1), (2.2), (2.4), (2.5), and (2.6) for temperatures along the heat pipe.

*Step 7 :* Solve Eq. (2.9) to determine the overall heat pipe heat transfer coefficient.

*Step 8 :* Calculate the view factors and the initial values.

*Step 9 :* Solve Eq. (3.1) with  $\zeta$  ranging from 0.0 to 1.0.

*Step 10 :* Solve Eqs. (2.22), (2.25), and (2.26) sequentially at each value of  $\zeta$  from 0.0 to 1.0. The fin midpoint temperature used in these equations is obtained from the initial values or from the previous iteration. There is, therefore, an ambiguity between the computed and the assumed midpoint temperatures. To remove this ambiguity, the solution to this set of equations was repeated using a fin midpoint temperature equal to the average between the computed and the assumed values.

*Step 11 :* Solve Eqs. (2.21), (2.32), and (3.3) with  $\zeta$  ranging from 0.0 to 1.0 and  $\theta$  from  $\theta_{\min}$  to  $\pi/2.0$

*Step 12 :* Test the solution for the requirement that the temperature gradient at the fin midpoint be 1.5 percent of the fin root temperature gradient or less. If the criteria was not met, the iteration is continued by returning to Step 6. The use of a similar criteria in the solution of the simple fin radiator resulted in an error in the fin efficiency of about one percent.

*Step 13 :* With updated value for  $T_{p,c}$ , calculate the new estimate for the required heat input.

*Step 14 :* Calculate the relative error using the new and previously obtained heat input estimates. If this error is less than a certain tolerance, the solution is converged and the calculated heat input is considered the correct match for the given operating temperature level. If the solution does not converge, update the value for the heat input and repeat the iteration sequence starting with *Step 4*.



## IV. RESULTS

The numerical results in this study were obtained by considering different heat pipe operating temperatures and then calculating the corresponding heat rejection requirements. The finite-difference scheme used a system of 100 increments along the fin and 30 increments around one-fourth of the heatpipe condenser circumference, assuming symmetry.

### 4.1 *Heat Transfer Coefficient of Heat Pipe Radiator*

Figure 4.1 shows the variation of the radiation parameter with respect to the temperature of the heat pipe condenser surface. Fig. 4.2 shows the total heat transfer rate of the heat pipe as a function of the operating temperature. Fig. 4.3 shows the temperature difference between the evaporator and the condenser surfaces of the heat pipe for various operating temperature levels. By using Eq.(2.9) the heat transfer coefficient of the heat pipe radiator was also determined as a function of the operating temperature level. The numerical results are tabulated in Tables C.1, C.2 and C.3 in Appendix C.

*4.1.1 Operating Temperature Effect:* As shown in Fig. 4.2, as the operating temperature increases so does the required heat transfer level. The temperature difference also follows a similar trend ( see Fig. 4.3 ), but the rate of increase was slightly slower. The temperature effect on the heat transfer coefficient is given in Fig. 4.4. It is interesting to note that the increase in heat transfer coefficient begins to level-off at approximately 400 K, reaching a value near 62,000. Also, as the operating temperature is raised, the radiation parameter increases, thus causing the fin efficiency to decrease, see Fig. 4.1.

*4.1.2 Heat Input Effect:* As the heat input increases with operating temperature, the overall temperature difference between the evaporator and the condenser also increases, see Fig. 4.3.

#### *4.2 Black Surfaces with Negligible Fin thickness*

Figure 4.5 shows the overall heatpipe-fin efficiency,  $\eta_{eff}$ , as a function of the radiation parameter ( $\beta_1$ ). The numerical results are included in Table C.4 of Appendix C, and compared well with the results of reference 14 in Figs. 4.9, 4.10, and 4.11 [14].

#### *4.3 Heat Pipe-Fin Radiator Efficiency*

As shown in Figs. 4.5, 4.6, 4.7, and 4.8, the heat pipe-fin radiator efficiency decreases as the radiation parameter increases. The radiation parameter is a function of condenser temperature which is determined from the given the operating temperature. For the given heat input, the radiation parameter increases with increasing operating temperature, and this has two opposing effects on the heat pipe-fin efficiency: (i) the heat is dissipated more in the section near the fin base than in the remaining section of the fin. (ii) Radiosity from the heat pipe condenser also increases, which means the irradiation on the fin increases, resulting in a higher fin temperature.

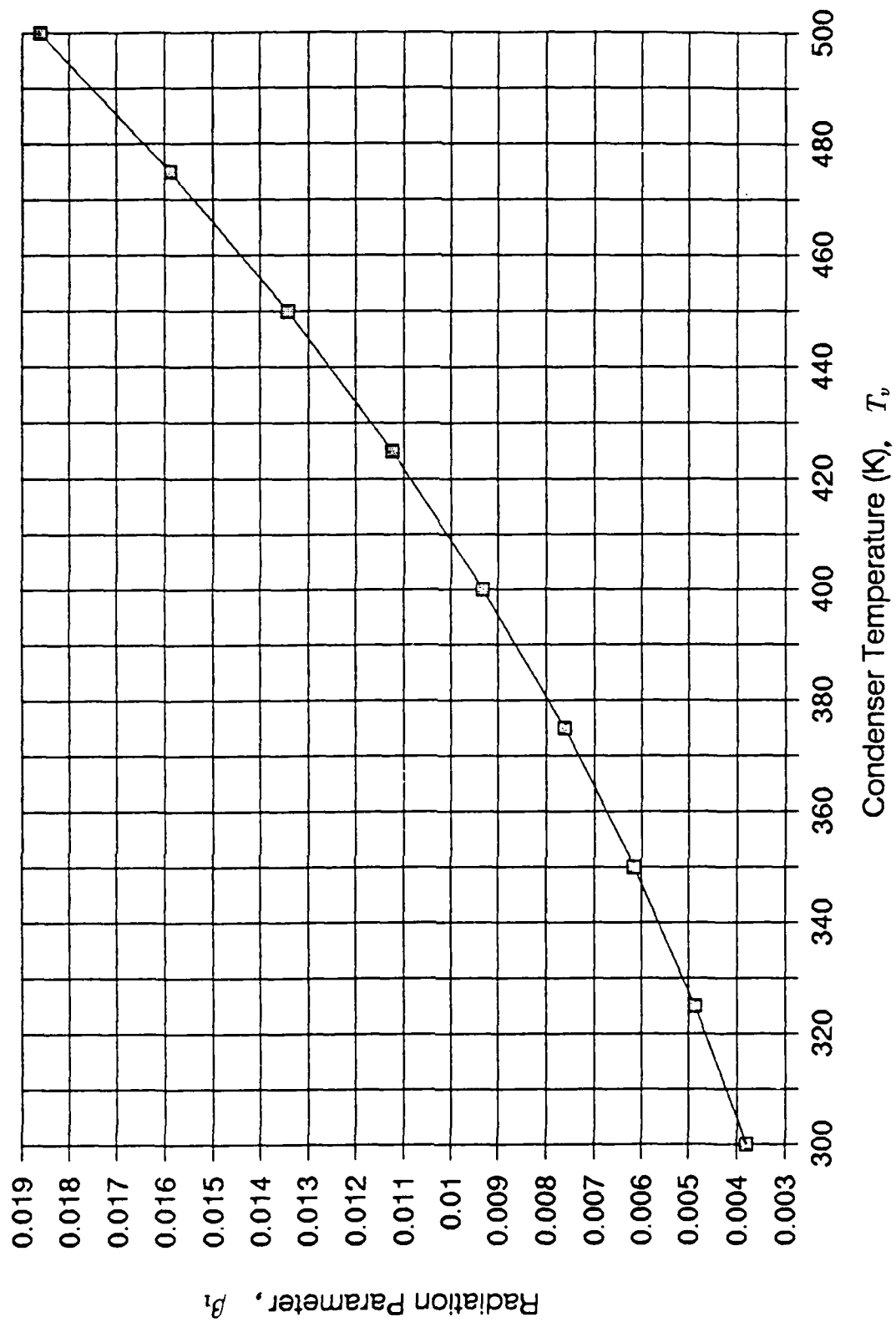


Figure 4.1. Relationship between Radiation Parameter and Operating Temperature

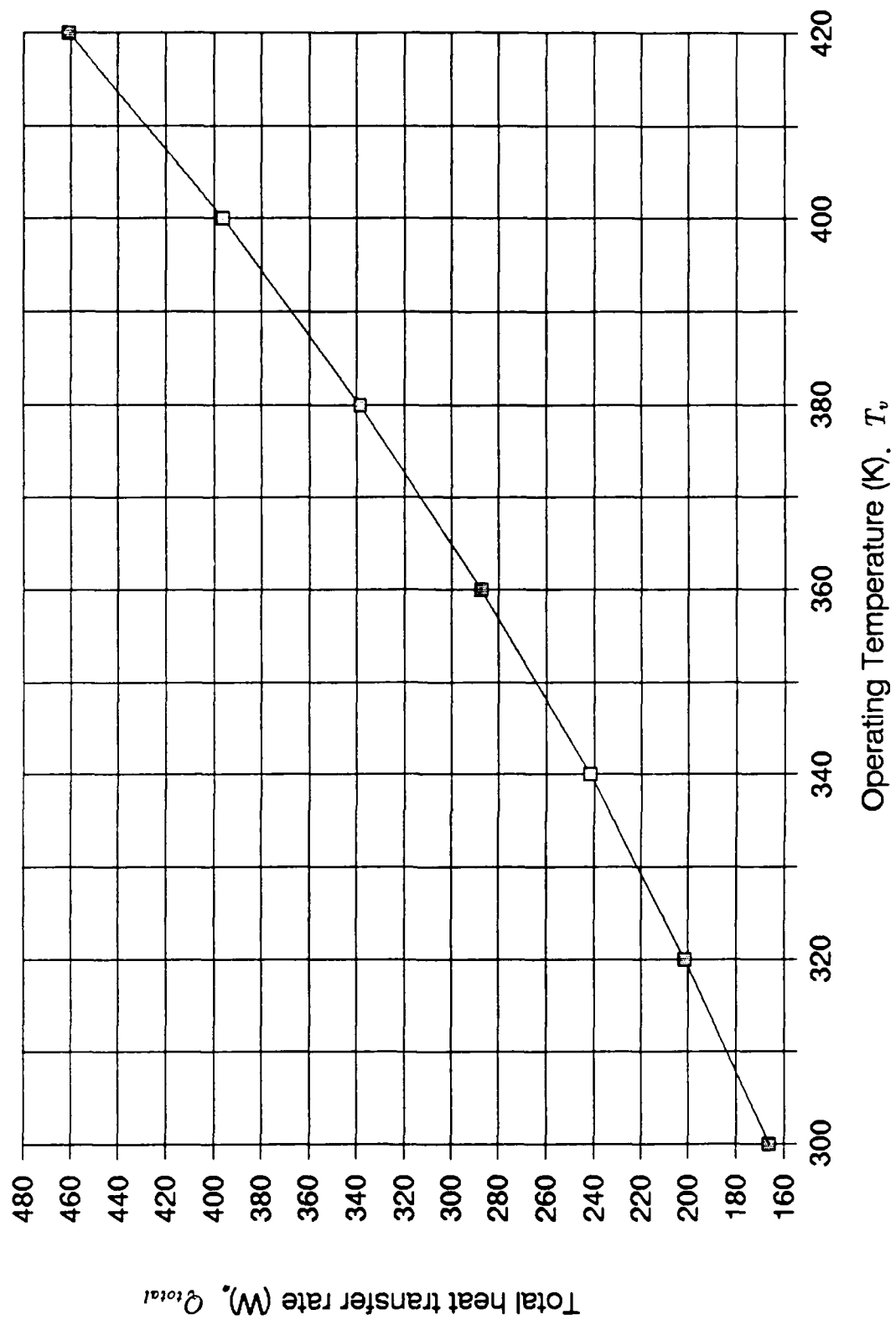


Figure 4.2. Total heat transfer rate of heat pipe vs. Operating Temperature

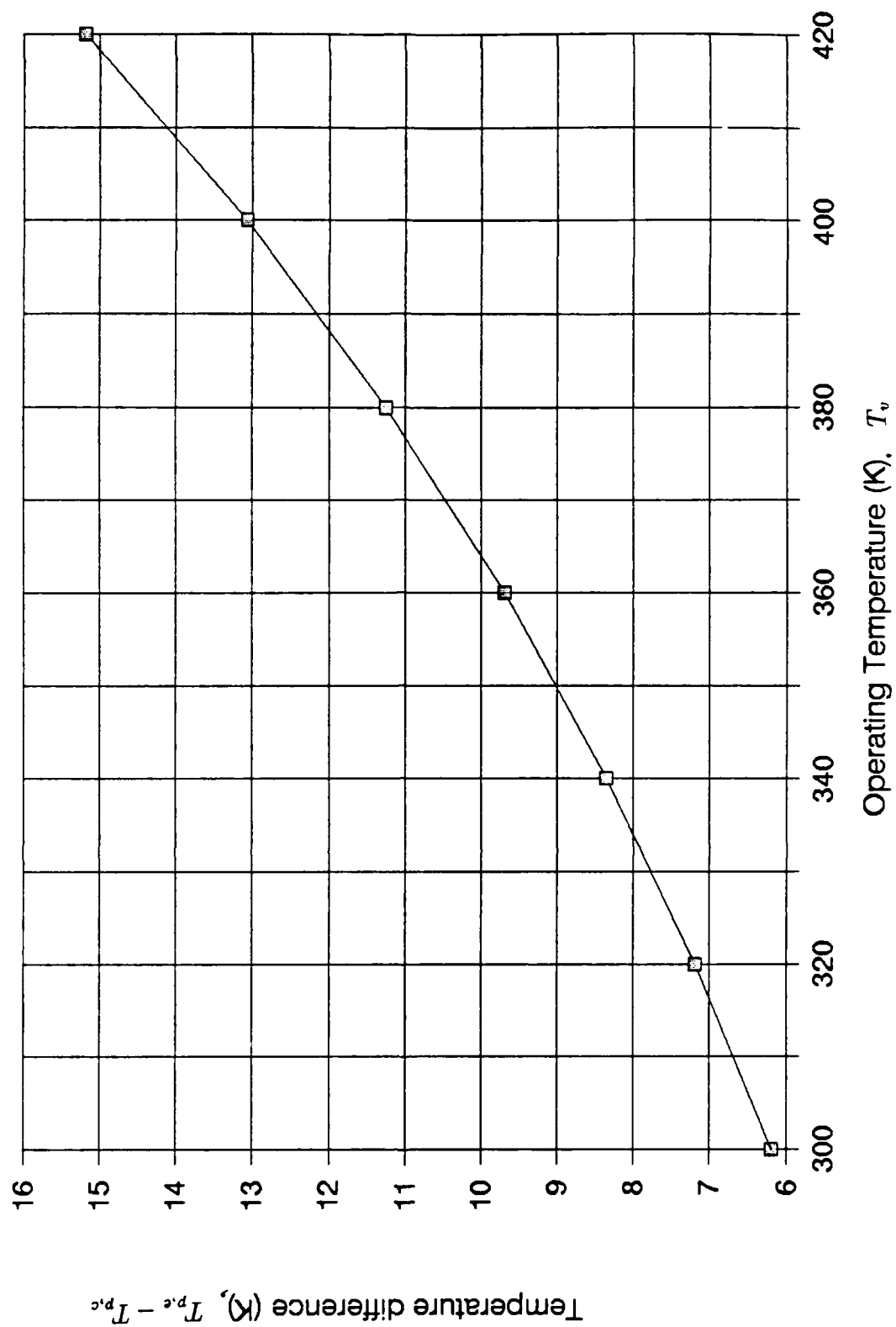


Figure 4.3. Temperature Difference between Evaporator and Condenser Temperature vs. Operating Temperature

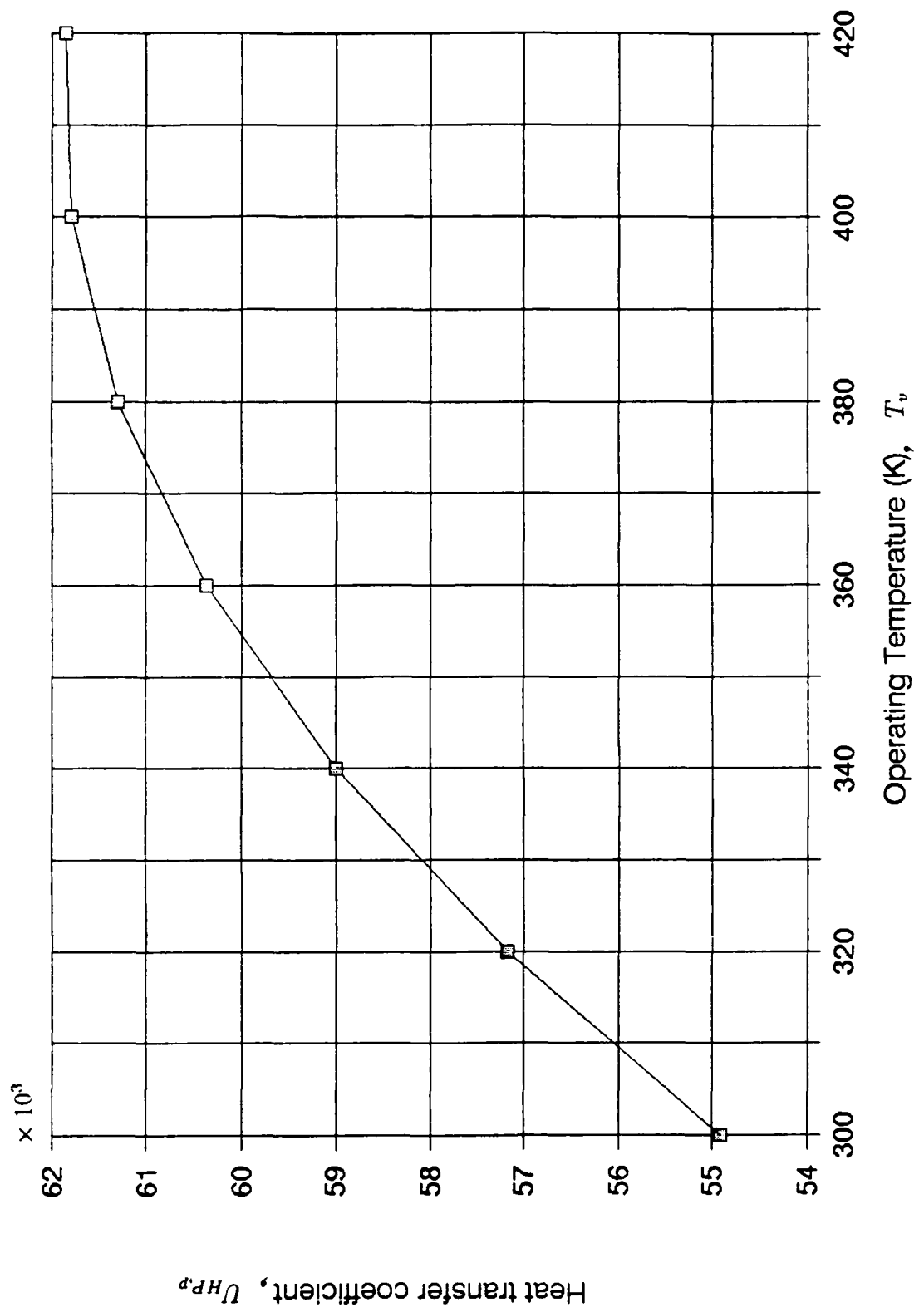


Figure 4.4. Overall heat transfer coefficient of heat pipe vs. Operating Temperature

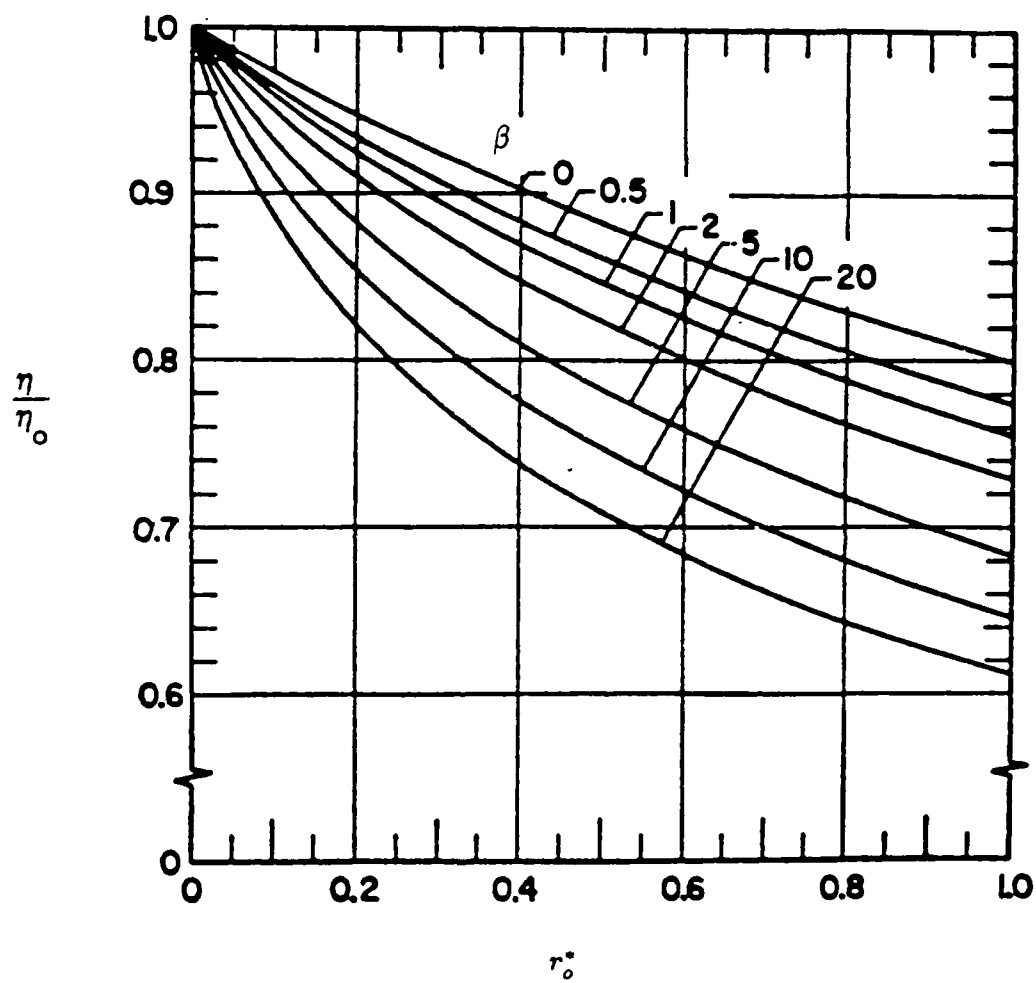


Figure 4.6. Condenser Surface Effects on Fin Heat Loss from Reference 14

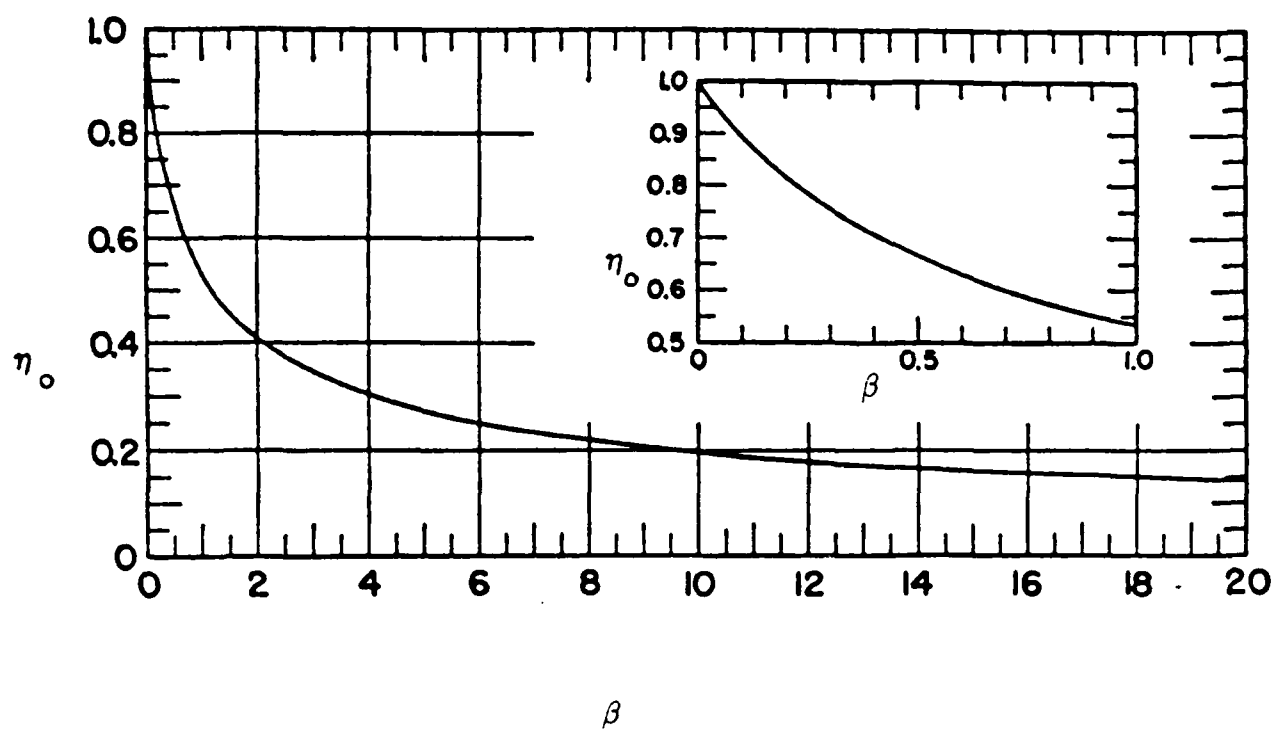


Figure 4.7. Simple Fin Efficiency from Reference 14



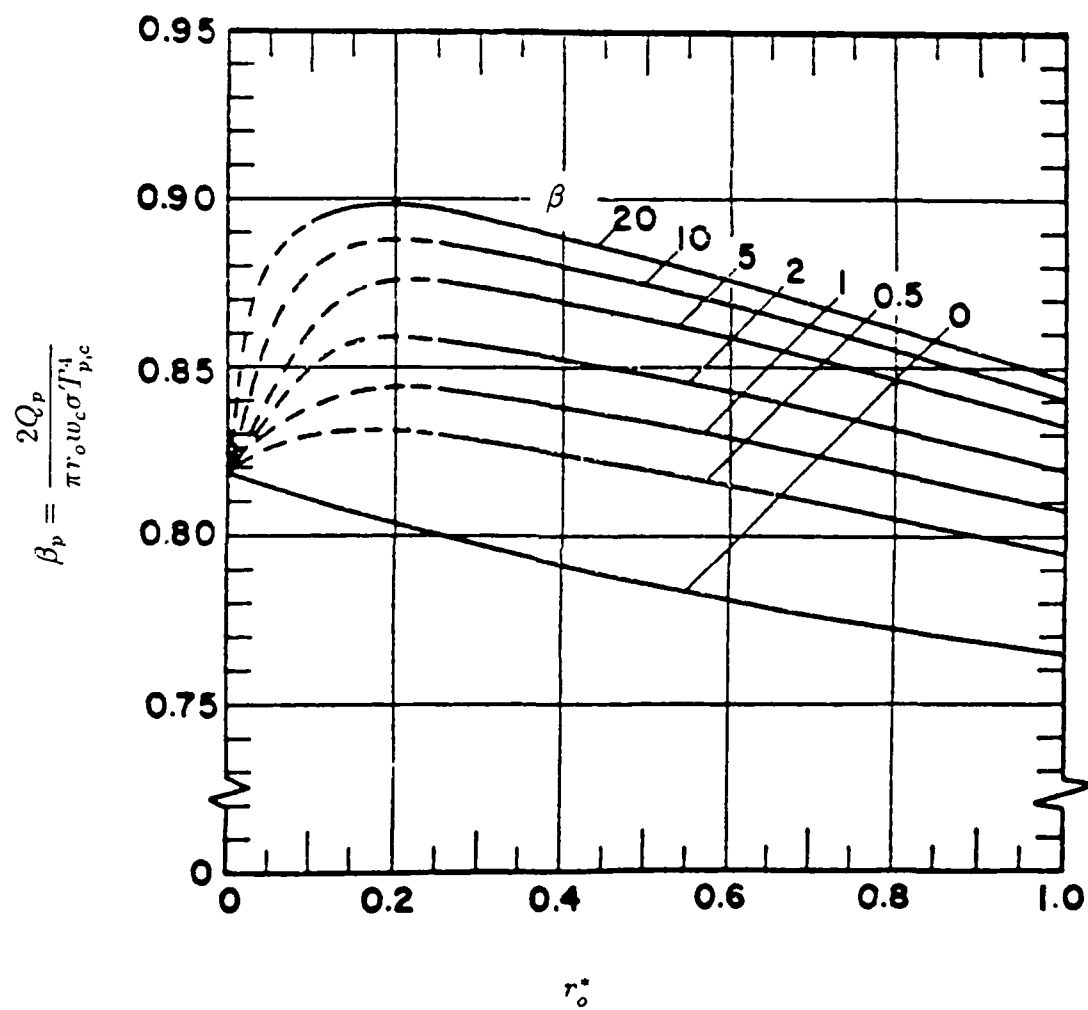


Figure 4.8. Condenser Surface Heat Loss from Reference 14

## *V. CONCLUSIONS AND RECOMMENDATIONS*

A mathematical analysis for a heat pipe radiator has been carried out to investigate fin efficiency and heat rejection requirements as a function of the heat pipe operating temperature. Grooved copper heat pipes with water as a working fluid, and copper fin, were considered for a given heat pipe operating temperature, the surface temperature of the evaporator and the condenser sections were calculated, along with the required heat rejection level.

From the evaluated condenser surface temperature, the radiation parameter and in turn, the fin efficiency were found. It was found that the overall temperature difference between the evaporator and the condenser increases as the operating temperature increases. As the condenser temperature increases, the radiation parameter increases while the fin efficiency decreases.

It is recommended to perform a more involved parametric study by using different dimensions of heat pipes and fins. Various vapor flow conditions, such as incompressible turbulent, compressible laminar, and compressible turbulent, may be included. Furthermore, different wick structures for the heat pipe may be incorporated, including screens, metal fibers, and metal powders. The existing computer program was written in a general fashion to facilitate condition changes for an effective parametric study.

Appendix A. *FORTRAN PROGRAM*

\*\*\*\*\*

\*

\*       FORTRAN   PROGRAM LISTING

\*

\*\*\*\*\*

\*       VARIABLE   DEFINITIONS

\*\*\*\*\*

\*

*     CKL	THERMAL CONDUCTIVITY OF LIQUID AT CONDENSER [ W / M*K ]
*     CKP	THERMAL CONDUCTIVITY OF HEATPIPE MATERIAL
*	AT CONDENSER [ W / M*K ]
*     CKW	THERMAL CONDUCTIVITY OF WICK MATERIAL AT CONDENSER
*	[ W / M*K ]
*     EKL	THERMAL CONDUCTIVITY OF LIQUID AT EVAPORATOR [ W / M*K ]
*     EKP	THERMAL CONDUCTIVITY OF HEATPIPE MATERIAL
*	AT EVAPORATOR [ W / M*K ]
*     EKW	THERMAL CONDUCTIVITY OF WICK MATERIAL AT EVAPORATOR
*	[ W / M*K ]
*     ETG	INITIAL GUESS VALUE OF OVERALL EFFICIENCY
*     FLEN	FIN LENGTH [ M ]
*     PKPC	THERMAL CONDUCTIVITY OF HEAT PIPE CONDENSER [ W / M*K ]
*     RI	HEATPIPE INSIDE RADIUS [ M ]
*     RRO	HEATPIPE OUTSIDE RADIUS [ M ]
*     RV	HEATPIPE VAPOR CORE RADIUS [ M ]
*     W	GROOVE WIDTH [ M ]
*     WA	LENGTH OF HEAT PIPE ADIABATIC SECTION [ M ]
*     WC	LENGTH OF HEAT PIPE CONDENSER [ M ]
*     WD	GROOVE DEPTH [ M ]
*     WE	LENGTH OF HEAT PIPE EVAPORATOR [ M ]
*     WF	LENGTH OF GROOVE FIN
*     NG	NUMBER OF RECTANGULAR GROOVES
*     TS	TEMPERATURE OF SPACE ENVIRONMENT [ K ]
*     Q	TOTAL REQUIRED HEAT REJECTION [ W ]
*     SIGMA	STEFAN-BOLTZMANN CONSTANT : 5.670E-08 [ W / M**2 K**4 ]
*     NHP	NUMBER OF HEAT PIPE IN MULTIPLE HEAT PIPE RADIATORS
*     QREQ	HEAT TRANSFER RATE IN SINGLE HEAT PIPE [ W ]
*     TPC	CONDENSER PIPE WALL TEMPERATURE [ K ]
*     PKEE	EFFECTIVE THERMAL CONDUCTIVITY OF LIQUID-SATURATED WICK
*	AT EVAPORATOR [ W / M*K ]
*     TPWE	EVAPORATOR TEMPERATURE AT PIPE-WICK INTERFACE [ K ]
*     TWVE	EVAOPRATOR TEMPERATURE AT WICK-VAPOR INTERFACE [ K ]
*     TVE	VAPOR TEMPERATURE IN EVAPORATOR [ K ]
*     VISCOSV	VAPOR DYNAMIC VISCOSITY [ KG / S*M ]
*     VDENS	VAPOR DENSITY [ KG / M**3 ]
*     TV	VAPOR TEMPERATURE [ K ]

* HFG	LATENT HEAT OF VAPORIZATION [ J / KG ]
* AREAV	VAPOR CORE CROSS-SECTIONAL AREA [ M**2 ]
* AREAP	HEAT PIPE CROSS-SECTIONAL AREA [ M**2 ]
* AREAC	CONDENSER SURFACE AREA OF HEAT PIPE
* FV	FRICTIONAL COEFFICEINT FOR VAPOR FLOW
* PDELTA	VAPOR PRESSURE DROP [ N / M**2 ]
* TVC	VAPOR TEMPERATURE IN CONDENSER [ K ]
* TWVC	CONDENSER TEMPERATURE AT WICK-VAPOR INTERFACE [ K ]
* PKEC	EFFECTIVE THERMAL CONDUCTIVITY OF LIQUID-SATURATED WICK AT CONDENSER [ W / M*K ]
* TPWC	CONDENSER TEMPERATURE AT WICK-PIPE INTERFACE [ K ]
* TPCNEW	NEW CONDENSER PIPE WALL TEMPERATURE [ K ]
* EPSIP	EMISSIVITY OF HEAT PIPE WALL SURFACE [ DIMENSIONLESS ]
* THICK	FIN THICKNESS [ M ]
* BETA1	RADIATION PARAMETER [ DIMENSIONLESS ]
* UHPP	HEAT TRANSFER COEFFICIENT BASED ON 'AREAP' [ W/M**2-K ]
* EPSIF	EMISSIVITY OF FIN SURFACE [ DIMENSIONLESS ]
* NFIN	NUMBER OF FIN NODES
* NPIPE	NUMBER OF HEAT PIPE NODES
* TSTAR	RATIO OF FIN NODE TEMPERATURE TO CONDENSER HEAT PIPE WALL TEMPERATURE
* RSTAR	TATIO OF HEAT PIPE OUTSIDE RADIUS TO HALF LENGTH OF FIN
* RHOP	REFLECTIVITY OF HEAT PIPE WALL SURFACE
* RHOF	REFLECTIVITY OF FIN SURFACE
* VFPP	VIEW FACTOR FROM FIN SEGMENT TO HEAT PIPE SEGMENT
* VFPP	VIEW FACTOR FROM HEAT PIPE SEGMENT TO HEAT PIPE SEGMENT
* TF	FIN NODE TEMPERATURE
* FIRRAD	IRRADIATION ON THE FIN AT FIN NODES
* FRAD	RADIOSITY FROM THE FIN
* PRAD	RADIOSITY FROM THE HEAT PIPE
* TEMISMP	TOTAL EMISSION FROM THE HEAT PIPES TO THE FIN MIDPOINT
* TEDGE	MIDPOINT TEMPERATURE OF FIN
* RATIO	RATIO OF TEMPERRATURE GRADIENT AT THE MID FIN TO THE ROOT TEMPERATURE GRADIENT
* RF	REDUCTION FACTOR
* T2IRRAD	TOTAL IRRADIATION ON A SEGMENT OF ONE HEAT PIPE FROM THE OTHER HEAT PIPE
* TIRRAD	TOTAL IRRADIATION ON A HEAT PIPE SEGMENT FROM THE FIN
* QTIRRAD	TOTAL IRRADIATION ON THE HEAT PIPE PER UNIT RADIUS
* ETAEFF	EFFICIENCY OF HEATPIPE-FIN RADIATOR
* ETAEFF	EFFICIENCY OF FIN ONLY

\*\*\*\*\*

\*            DIMENSIONS AND FORMATS

\*\*\*\*\*

\*

```
REAL  RRO,TPC,EKL,EKP,TV,VDENS,VISCOV,HFG,TWVC,CKL,CKP,PKPC,WF
REAL  RI,RV,WE,WA,WC,W,WD,TS,TPE,Q,FLEN,THICK,EPSIP,EPSIF
REAL  BETA,BETA1,UHPP,PDELTA
REAL  VSINE(31),VCOSIN(31),VFPP(101,31),VFPP(31,31),TF(101)
REAL  GRADT(101),GRADT2(101),FIRRAD(101),FRAD(101),PRAD(101)
INTEGER PIPENO,FINNO,NG,NHP,NFIN,NPIPE
```

\*

```
OPEN(UNIT=3,FILE='PIP1.DAT',STATUS='OLD')
OPEN(UNIT=6,FILE='PIP2.DAT',STATUS='NEW')
READ(3,91) RRO,RV
READ(3,90) WE,WA,WC
READ(3,91) W,WD
READ(3,92) NG,NHP
READ(3,90) TS,TV,ETG
READ(3,91) FLEN,THICK
READ(3,91) EPSIP,EPSIF
READ(3,92) NFIN,NPIPE
90 FORMAT(3F12.6)
91 FORMAT(2F12.6)
92 FORMAT(2I5)
```

\*\*\*\*\*

\*            CONSTANTS

\*\*\*\*\*

\*

```
TPCG = TV
PI = 3.141593
HFLEN = FLEN/2.
HTHICK = THICK/2.
SIGMA = 5.670E-8
RI = RV + WD
WF = ( PI*(RI+RV)/FLOAT(NG)) - W
QTT1 = (SIGMA*TPCG**4.*(HFLEN+SQRT(RRO**2.-HTHICK**2.))*WC)
QREQ = 4.*ETG*QTT1
PRINT*, QREQ
799 CONST1 = RRO/RI
CONST2 = RI/RV
CONSTA = ( LOG(CONST1) * QREQ ) / ( 2.0*PI )
CONSTB = ( LOG(CONST2) * QREQ ) / ( 2.0*PI )
AREAV = PI*RV**2
AREAP = FI*RRO**2
AREAC = 2.0*PI*RRO*WC
```

```

*****
*
*   PART 1 : HEAT PIPE CONDITIONS
*
*****
*
*.....CALCULATE PROPERTIES & PRESSURE DROP
*           AT VAPOR TEMPERATURE

          CALL STEAMDEN(TV,VDENS)
          CALL STEAMUG(TV,VISCOV)
          CALL STEAMHFG(TV,HFG)

*.....
          FV = ( 8.0*VISCOV ) / ( HFG*VDENS*AREAV*RV**2 )
          PDELTA = FV*QREQ*( WE/6.0 + WA + WC/6.0 )

*.....CALCULATE TEMPERATURE AT EVAPORATOR

          TVC = TV
          TVE = TVC + ( TV*PDELTA ) / ( VDENS*HFG )
          TWVE = TVE

*.....CALCULATE CONDUCTIVITY & TEMPERATURE AT EVAPORATOR
          CALL WATER(TWVE,EKL)
          CALL COPPER(TWVE,EKP)
          EKW = EKP
          PKW = 0.185*WF*EKW + WD*EKL
          PKEE = (WD*WF*EKL*EKW + W*EKL*PKW) / ((W+WF)*PKW)
          TPWE = TWVE + CONSTB / ( PKEE*WE )
          CALL COPPER(TPWE,EKP)
          EKW = EKP
          TPE = TPWE + CONSTA / ( EKP*WE )

*.....CALCULATE TEMPERATURE AT CONDENSER

          TVC = TV
          TWVC = TVC
          CALL WATER(TWVC,CKL)
          CALL COPPER(TWVC,CKP)
          CKW = CKP
          PKEC = ( W*CKL + WF*CKW )/( W + WF )
          TPWC = TWVC - CONSTB / ( PKEC*WC )
          TPC = TPWC - CONSTA / ( CKP*WC )

          CALL COPPER(TPC,CKP)

```

```

CALL COPPER(TPC,PKPC)

UHPP = ( QREQ ) / (( TPE - TPC ) * AREAP )
BETA1 = ( SIGMA*(TPC**3)*(HFLEN**2)*EPSIP ) / ( PKPC*HTHICK )
BETA = BETA1*EPSIF
*.....
WRITE(6,20) RRO,RI,RV
20 FORMAT(1X,'RRO =',F8.2, 5X,'Ri =',F8.2,5X,'Rv =',F8.2)
WRITE(6,21) FLEN,THICK
21 FORMAT(1X,'FLEN =',F8.2, 5X,'THICK =',F8.2)
WRITE(6,22) WE,WA,WC
22 FORMAT(1X,'WE =',F8.2, 5X,'WA =',F8.2,5X,'WC =',F8.2)
WRITE(6,23) W,WD,NG
23 FORMAT(1X,'W =',F8.2, 5X,'WD =',F8.2,5X,'NG =',I3)
WRITE(6,24) EPSIF,EPSIP
24 FORMAT(1X,'EPSIF =',F8.2, 5X,'EPSIP =',F8.2)
WRITE(6,25) NFIN,NPIPE,NHP
25 FORMAT(1X,'NFIN =',I3, 5X,'NPIPE =',I3,5X,'NHP =',I3)
WRITE(6,26) TPE,TS,Q
26 FORMAT(1X,'TPE =',F8.2, 5X,'TS =',F8.2,5X,'Q =',F8.2)
WRITE(6,38)
WRITE(6,39) TPE,TPWE,TVE,TV,TPWC,TVC,TPC
WRITE(6,40) TPE,TPC
WRITE(6,41) BETA1,UHPP,PDELTA
WRITE(6,42)
WRITE(6,43) TPE,EKP,EKL,TPWE,TVE
WRITE(6,45) TEMPDIFF,BETA1,UHPP,PKPC
WRITE(6,44)
WRITE(6,46) TV,HFG,TVC,TPWC,TPC
38 FORMAT(8X,'TPE',6X,'TPWE',7X,'TVE',8X,'TV',6X,'TPWC',7X,'TVC',
1 7X,'TPC'5X)
39 FORMAT(1X, 7(2X,F8.2))
40 FORMAT(1X,'EVAPORATOR TEMP =',F8.2,5X,'CONDENSER TEMP =',F8.2)
41 FORMAT(1X,'RADIATION PARAMETER =',F8.2, 5X,'HEAT TRANS COEFF =',
1 F18.2, 5X,'PRESSURE DROP =',F8.2)
42 FORMAT(1X,'TPE, EKP, EKL, TPWE, TVE,TEMPDIFF, BETA1, UHPP, PKPC')
43 FORMAT( 1X,F8.2, 4(4X,F18.2) )
44 FORMAT(1X,'TV, VDENS, VISCOSV, HFG, TVC, CKP, CKL, TPWC, TPC')
45 FORMAT(1X, 4(4X,F8.2) )
46 FORMAT(1X, 5F15.2)

```



```

*****
*
*   PART 2 : HEATPIPE - FIN RADIATION
*
*****
*
*****
*   CONSTANTS RELATED HEATPIPE-FIN
*****
    RSTAR = RRO / HFLEN
    TSTAR = HTHICK / HFLEN
    PARAA = DSQRT( 0.4DO*BETA )
    RHOP = 1.0 - EPSIP
    RHOF = 1.0 - EPSIF
    PIPENO = NPIPE - 1
    FINNO = ( NFIN - 1 ) / 2
    NFIN1 = NFIN - 1
    NFIN2 = ( NFIN + 1 ) / 2
    NDFIN = NFIN / 8
    NDFIN2 = NFIN / 20
    NFIN3 = NFIN2 - NDFIN2
    NDPIPE = NPIPE / 9
    ZETAD = 1.0DO / FLOAT(FINNO)
    P = SQRT( RSTAR**2 - TSTAR**2 )
    THETAMIN = ATAN( TSTAR / P )
    THETAD = ( PI/2.0 - THETAMIN ) / PIPENO
    THETAD2 = 0.5 * RSTAR * THETAD
    THETAD3 = THETAMIN + ( THETAD / 4.75 )
    ARCONST = FINNO * THETAD * RSTAR
    THETA = THETAMIN

*.....
    NCOUNT = 1
    VSINE(1) = SIN( THETAD3 )
    VCOSIN(1) = COS( THETAD3 )
    DO 200 J=2, NPIPE
        THETA = THETA + THETAD
        VSINE(J) = SIN( THETA )
        VCOSIN(J) = COS( THETA )
    200 CONTINUE

```

```

*****
*   VIEW FACTOR FROM FIN SEGMENT TO
*   PIPE SEGMENT ( VFPF )
*****
*
300 QJ3 = 0.0
*
DO 329 J=1, NPIPE
IF ( QJ3 ) 326, 321, 321
321 THICKTAN = ( TSTAR * VSINE(J) ) / VCOSIN(J)
AJ3 = RSTAR * VSINE(J) - TSTAR
BJ31 = THICKTAN + RSTAR * VCOSIN(J)
BJ32 = ( TSTAR / VCOSIN(J) ) * ( TSTAR / VCOSIN(J) )
S = P + THICKTAN + ( ZETAD / 5.0 )
AXJ3 = S * VCOSIN(J) - TSTAR
AXJ4 = AJ3 * AXJ3
*
IF ( AXJ4 ) 327, 328, 328
327 VFPF(1,J) = 0.0
QJ3 = - 1.0
GO TO 329
328 B3 = 2.0 * (( S**2 - 2.0*S*BJ31 + RSTAR**2 + BJ32 )** 1.5 )
VFPF(1,J) = ( AXJ4 / B3 ) * ZETAD

GO TO 329
326 VFPF(1,J) = 0.0
329 CONTINUE
*
QJ3 = 0.0
*
DO 311 J=1, NPIPE
QX3 = 0.0
IF ( QJ3 ) 9999, 301, 309
301 THICKTAN = ( TSTAR * VSINE(J) ) / VCOSIN(J)
AJ3 = RSTAR * VSINE(J) - TSTAR
BJ31 = THICKTAN + RSTAR*VCOSIN(J)
BJ32 = ( TSTAR / VCOSIN(J) ) * ( TSTAR / VCOSIN(J) )
*
DO 308 M=1, NFIN1
IF ( QX3 ) 9999, 302, 307
302 L = NFIN + 1 - M
LX = L - 1
S = P + THICKTAN + LX*ZETAD

AXJ3 = S * VCOSIN(J) - TSTAR

```

```

      AXJ4 = AJ3 * AXJ3
*
      IF ( AXJ4 ) 304, 303, 303
303  B3 = 2.0 * ( ( S**2 - 2.0*S*BJ31 + RSTAR**2 + BJ32 )**1.5 )
      VFPP(L,J) = ( AXJ4 / B3 ) * ZETAD
      GO TO 308
*
304  IF ( LX - 2*FINNO ) 306, 305, 9999
305  QJ3 = 1.0
306  QX3 = 1.0
307  VFPP(L,J) = 0.0
*
308  CONTINUE
      GO TO 311
*
309  DO 320 L=1, NFIN
      VFPP(L,J) = 0.0
320  CONTINUE
311  CONTINUE
      SUMVF1 = 0.0
*
      DO 313 N=2, NFIN
      SUMVF1 = VFPP(N,1) + SUMVF1
313  CONTINUE
      VBETA1 = ATAN( (RSTAR*VSINE(1)) / (2.0 + P - RSTAR*VCOSIN(1)))
      GAMMA = 1.5708 - VBETA1 - THETAD3
      VFPP(1,1) = 1.0 - COS(GAMMA) - 2.0*SUMVF1 + VFPP( NFIN, 1 )

```

```

*****
*   VIEW FACTOR FROM HEAT PIPE TO
*   HEAT PIPE ( VFPP )
*****
*
*
350 DO 357 J=1,NPIPE
    QK3B = 0.0
*
    DO 357 K=1, NPIPE
    IF ( J - K ) 361, 361, 362
*
361 IF ( QK3B ) 9999, 351, 356
351 A351 = ( VSINE(J) - VSINE(K) ) * RSTAR
    B351 = ((1.0 + P)*2.0) - ( RSTAR*( VCOSIN(J) + VCOSIN(K) ) )
    E351 = ( B351 * VCOSIN(J) - A351*VSINE(J) )*( B351 * VCOSIN(K) -
1 A351 * VSINE(K) )
*
    IF ( E351 ) 354, 353, 353
353 C351 = THETAD2 / ( ( A351 **2 + B351 **2 )** 1.5 )
    VFPP(J,K) = E351 * C351
    GO TO 357
354 QK3B = 1.0
356 VFPP(J,K) = 0.0
    GO TO 357
362 VFPP(J,K) = VFPP(K,J)
357 CONTINUE
    DO 363 J=1, NPIPE
    VFPP(J,1) = 0.5 * VFPP(J,1)
363 CONTINUE
*
*****
*   EDGE TEMPERATURE -- BLACK SIMPLE FIN
*****
*
299 TEDGE = ((( ( -2.2001614E-6 * BETA + 1.7217342E-4 ) * BETA -
1 4.3974392E-3 ) * BETA + 4.6408689E-2 ) * BETA - 0.22322417 )
2 * BETA + 0.95864883
*
*****
*   INITIAL CHARACTERISTICS
*****
*
    TEMISMP = 0.0

```

```

100 DO 101 J=2, NPIPE
    TEMISMP = VFPP( NFIN2, J ) + TEMISMP
    PRAD(J) = EPSIP
101 CONTINUE
    TEMISMP = 2.0*ARCONST*EPSIP*(TEMISMP + 0.5*VFPP(NFIN2,1))
    PRAD(1) = 0.5 * EPSIP
*
    IF ( TEDGE**4 - TEMISMP ) 103, 104, 104
103 TEDGE = TEMISMP ** 0.25
104 TEDGE5 = TEDGE ** 5
    TEC = - 1.0
    I = 1
    TF(I) = 1.0
106 IF ( TEC ) 111, 112, 112
111 TGRAD = ( TF(I) ** 5 ) - TEDGE5
*
    IF ( TGRAD ) 107, 107, 108
107 GRADT(I) = 0.0
    TEC = TF(I)
    GO TO 109
112 TF(I) = TEC
    GRADT(I) = 0.0
    GO TO 109
108 GRADT(I) = - PARAA * SQRT( TGRAD )
    TF(I+1) = TF(I) + GRADT(I) * ZETAD
109 I = I + 1
113 IF ( I - NFIN2 ) 106, 106, 399
399 PARAB = ( RSTAR * EPSIP ) / ( 1.0 + P )

```

```

*****
*               IRRADIATION
*****
*
400  DO 402 L=1, NFIN2
      FIRRAD(L) = 0.0
      M = NFIN + 1 - L
*
      DO 401 J=1, NPIPE
        FIRRAD(L) = PRAD(J) * ( VFPF(L,J) + VFPF(M,J) ) + FIRRAD(L)
401  CONTINUE
      FIRRAD(L) = ARCONST * ( FIRRAD(L) - 0.5*PRAD(1) * ( VFPF(L,1)
1 + VFPF(M,1)))

      IF ( NCOUNT - 10 ) 410, 411, 411
410  RF = NCOUNT
      FIRRAD(L) = RF * FIRRAD(L) / 10.000

411  CONTINUE
      FIRRAD(M) = FIRRAD(L)
402  CONTINUE
*
*****
*               FIN TEMPERATURE
*****
*
500  N5 = - 2
511  TI = 0.0
*
      DO 501 L=1, NFIN2
        TI = ( FIRRAD(L) * GRADT(L) ) + TI
501  CONTINUE
506  SUMIRRAD = 0.0
      P3 = 0.0
*
      DO 508 L=1, NFIN2
        T4 = TF(L) ** 4
        GRADT2(L) = BETA * ( T4 - FIRRAD(L) )
522  SUMIRRAD = ( FIRRAD(L) * GRADT(L) ) + SUMIRRAD
        GRAD = ( T4 * TF(L) ) - TEDGES + ( 5.0 * ZETAD*(TI - SUMIRRAD))
*
      IF ( GRAD ) 504, 504, 505
504  GRADT(L) = 0.0
      P3 = P3 + 1.0
      GO TO 508

```

```

505 GRADT(L) = - PARAA * SQRT( GRAD )
    TF(L+1) = TF(L) + GRADT(L) * ZETAD + 0.5*GRADT2(L)*( ZETAD**2 )
508 CONTINUE
    CALL COPPER(TPC,CKP)

    QFN =-CKP*WC*HTHICK*(GRADT(1)/4.)*TPC/HFLEN
    N5 = N5 + 1

    IF ( N5 ) 507, 511, 509
507  TEDGE = 0.5 * ( TF(NFIN2) + TEDGE )
    TEDGE5 = TEDGE ** 5
    GO TO 511
509  RATIO = GRADT( NFIN2 ) / GRADT( 1 )
    PR = RATIO
    P5 = TEDGE - TF( NFIN2 )
    RD = PR - RATIO
    NCOUNT = NCOUNT + 1
    TEDGE = TF( NFIN2 ) - P5
    TEDGE5 = TEDGE ** 5

```

\*\*\*\*\*

\*                   RADIOSITY

\*\*\*\*\*

\*

```
600 DO 601 L=1, NFIN2
    FRAD(L) = EPSIF * ( TF(L) ** 4 ) + RHOF * FIRRAD(L)
    M = NFIN + 1 - L
    FRAD(M) = FRAD(L)
601 CONTINUE
    QTIRRAD = 0.0
```

\*

```
DO 604 J=1, NPIPE
    TIRRAD = 0.0
```

\*

```
DO 602 L=1, NFIN
    TIRRAD = FRAD(L) * VFPP(L,J) + TIRRAD
602 CONTINUE
    TIRRAD = TIRRAD - 0.5DO * FRAD(1) * ( VFPP(1,J) + VFPP(NFIN,J) )
```

\*

```
T2IRRAD = 0.0DO
DO 603 K=1, NPIPE
    T2IRRAD = PRAD(K) * VFPP(J,K) + T2IRRAD
603 CONTINUE
    PRAD(J) = EPSIP + RHOP * ( TIRRAD + T2IRRAD )
    QTIRRAD = TIRRAD + T2IRRAD + QTIRRAD
604 CONTINUE
```

```
QC=QFN+SIGMA*TPC**4.*WC*RRO*(PI/2.-THETAMIN-(QTIRRAD/4.))
QTT1=SIGMA*TPC**4.*(HFLN+SQRT(RRO**2.-HTHICK**2.))*WC
ETAEFF1=QC/QTT1
QDIV=ABS(((QREQ/4.)-QC)/QC)
WRITE(6,*) QDIV,QREQ,QC,ETAEFF1
IF(QDIV.LE.1E-6) GO TO 899
QREQ=4.* QC
GO TO 799
```

\*

\*\*\*\*\*

\*                   CRITEIA

\*\*\*\*\*

\*

```
IF ( NCOUNT - 15 ) 400, 400, 704
704 IF ( NCOUNT - 100 ) 705, 800, 800
705 IF ( ABS( RATIO ) - 0.015 ) 706, 800, 400
706 IF ( P3 - 1.0 ) 800, 800, 400
```



```

*
*****
*           EFFICIENCY
*****
*
899  CALL STEAMDEN(TV,VDENS)
      CALL STEAMHFG(TV,HFG)
      CALL COPPER(TV,EKP)
      CKP=EKP
      CALL WATER(TV,EKL)
      EKW=EKP
      PKW=.185*WF*EKW+WD*EKL
      PKEE=(WD*WF*EKL*EKW+W*EKL*PKW)/((W+WF)*PKW)
      CKW=CKP
      CKL=EKL
      PKEC=(W*CKL+WF*CKW)/(W+WF)
      DTT=CONSTA/(WE*EKP)+CONSTB/(WE*PKEE)+(TV*PDELTA)/(VDENS*HFG)
*      +CONSTB/(WC*PKEC)+CONSTA/(WC*CKP)
      UHP=QREQ/(DTT*PI*RR0**2)
      WRITE(6,*) DTT,UHP
800  ETAFIN = - GRADT(1) / BETA1
      ETAEFF = PARAB *(1.5708DO - THETAMIN - (QTIRRAD* THETAD))
1 + ( ETAFIN / ( 1.0DO + P ))
      RN = RSTAR * ( BETA1 ** 0.3333 )
      COUNT = NCOUNT

```

\*\*\*\*\*

\*                   OUTPUTS

\*\*\*\*\*

\*

\*.....

```
WRITE(6,952) TEDGE,P5,GRADT(1),GRADT(NFIN2),RATIO
WRITE(6,903) TSTAR,RSTAR,EPSIP,EPSIF,BETA1,ETAEFF,ETAFIN,COUNT
WRITE(6,911)
WRITE(6,902) ( TF(N), N=1, NFIN2, NDFIN2 )
WRITE(6,912)
WRITE(6,902) ( GRADT(N), N=1, NFIN2, NDFIN2 )
WRITE(6,913)
WRITE(6,902) ( GRADT2(N), N=1, NFIN2,NDFIN2 )
WRITE(6,914)
WRITE(6,902) ( FIRRAD(N), N=1, NFIN2, NDFIN2 )
WRITE(6,915)
WRITE(6,902) ( FRAD(N), N=1, NFIN2, NDFIN2 )
WRITE(6,916)
WRITE(6,902) ( PRAD(J), J=1, NPIPE, NDPIPE )
WRITE(6,903) RD, TI, TEMS, QTIRRAD, FINNO, PIPENO, RN, BETA
WRITE(6,904) P,ARCONST,THETAMIN,PARAB,ZETAD,THETAD,THETAD3
```

\*.....

```
901 FORMAT( 1X, 10F12.8)
902 FORMAT( 1X, 11F10.6)
903 FORMAT( 1X, 4F14.8,2I5,2F14.8)
904 FORMAT( 1X, 7F14.8)
911 FORMAT( 1X, 'TEMPERATURE', 2X, 'DISTRIBUTION' )
912 FORMAT( 1X, 'TEMPERATURE',2X, 'GRADIENT',2X, 'DISTRIBUTION')
913 FORMAT( 1X, 'SECOND', 2X, 'DERIVATIVE', 2X,'OF', 2X,
1 'TEMPERATURE' )
914 FORMAT( 1X, 'IRRADIATION',2X,'ON', 2X,'FIN' )
915 FORMAT( 1X, 'FIN', 2X, 'RADIOSTY' )
916 FORMAT( 1X, 'TUBE', 2X, 'RADIOSTY' )
952 FORMAT( 1X, 'EDGE TEMP=', F9.6, 5X, 'P=',F9.6, 5X,
1 'ROOT GRAD=', F9.6, 5X, 'TIP TEMP GRAD=', F9.7,
2 5X, 'GRAD RATIO=', PE10.3 )
981 FORMAT( 1X, 6F14.8)
```

\*

```
CLOSE(UNIT=3)
CLOSE(UNIT=6)
GO TO 9999
```

\*

```
9999 STOP
END
```

```

*****
*      SUBROUTINE  WATER                      *
*                                                    *
*      FIND CONDUCTIVITY OF WATER              *
*      BY USING LEAST SQUARES METHOD          *
*****

```

SUBROUTINE WATER(T,WK)

DOUBLE PRECISION WK  
REAL WK

AA = -0.3985D6  
BA = 0.5282D4  
CA = -0.6389D1  
WK =(AA + BA\*T + CA\*T\*T)\*1E-6  
RETURN  
END

```

*****
*      SUBROUTINE  COPPER                      *
*                                                    *
*      FIND CONDUCTIVITY OF COPPER              *
*      BY USING LEAST SQUARES METHOD          *
*****

```

SUBROUTINE COPPER(T,CC)

DOUBLE PRECISION CC  
REAL CC

AB = 0.3799D3  
BB = -0.3780D-1  
CB = 0.1023D5  
CC = AB + BB\*T + CB / T  
RETURN  
END

```

*****
*      SUBROUTINE STEAMDEN                      *
*                                                                 *
*      FIND DENSITY OF STEAM                      *
*      BY USING LEAST SQUARES METHOD              *
*****

```

SUBROUTINE STEAMDEN(T,DENSITY)

DOUBLE PRECISION DENSITY,SV  
 REAL DENSITY,SV

AC = 0.3956D-6  
 BC = 0.9677D3  
 SV = AC\*T +( BC/T )  
 DENSITY = 1 / SV  
 RETURN  
 END

```

*****
*      SUBROUTINE STEAMHFG                      *
*                                                                 *
*      FIND LATENT HEAT OF WATER VAPORIZATION*
*      BY USING LEAST SQUARES METHOD              *
*****

```

SUBROUTINE STEAMHFG(T,HEATLATENT)

DOUBLE PRECISION HEATLATENT  
 REAL HEATLATENT

AD = 0.1022D4  
 BD = 0.9197D1  
 CD = -0.1531D-1  
 HEATLATENT = (AD + BD\*T + CD\*T\*T)\*1E3  
 RETURN  
 END

```

*****
*      SUBROUTINE  STEAMUG                      *
*                                                    *
*      FIND VISCOSITY OF STEAM                  *
*      BY USING LEAST SQUARES METHOD            *
*****

```

```

SUBROUTINE  STEAMUG(T,VISCOSITY)

```

```

DOUBLE PRECISION  VISCOSITY
REAL              VISCOSITY

```

```

AE = -0.2557D-7
BE =  0.4088D-4
VISCOSITY = (T / ( AE*T + BE ))*1E-12
RETURN
END

```

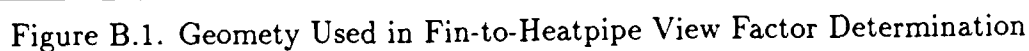
```

*****
*      CASE INPUT DATA                      *
*****

```

RR0 = 0.01	RV = 0.01	
WE = 0.15	WA = 0.05	WC = 1.50
NG = 50	NHP = 10	
TS = 0.0	TV = 300	ETG = 0.95
FLEN = 0.01	THICK = 0.005	
EPSIP = 1.0	EPSIF = 1.0	
NFIN = 101	NPIPE = 31	

Appendix B. *VIEW FACTOR EQUATIONS*



The geometry of the problem for evaluating the view factor from fin to heatpipe is shown in Fig.B.1 and the parameters are expressed in the non-dimensional terms which is divided by the half of fin length,  $L$  ,

$$\cos\theta = \frac{r_o^* + S_2^*}{L_1^*} = \frac{t^*}{S_4^*} \quad (\text{B.1})$$

$$L_1^* = [r_o^{*2} - t^{*2}]^{1/2} + \zeta + L_2^* \quad (\text{B.2})$$

$$\sin\theta = \frac{S_3^* + S_4^*}{L_1^*} = \frac{L_2^*}{S_4^*} \quad (\text{B.3})$$

$$\sin\psi = \frac{S_3^*}{S_1^*} \quad (\text{B.4})$$

$$S_1^{*2} = S_2^{*2} + S_3^{*2} \quad (\text{B.5})$$

$$\sin\psi = \frac{L_1^* \sin\theta - S_4^*}{[S_2^{*2} + S_3^{*2}]^{1/2}} \quad (\text{B.6})$$

Combining Eqs.(B.1),(B.3), and (B.6) yields

$$\sin\psi = \frac{u}{v} \quad (\text{B.7})$$

where

$$u = L_1^* \sin\theta - S_4^*$$

$$v = [L_1^{*2} - 2L_1^* \{r_o^* \cos\theta + S_4^* \sin\theta\} + r_o^{*2} + S_4^{*2}]^{1/2}$$

Combining Eqs.(B.1),(B.2), and (B.3) yields

$$L_1^* = [r_o^{*2} - t^{*2}]^{1/2} + \zeta + t^* \tan\theta \quad (\text{B.8})$$

From Eq.(B.7)

$$d(\sin\psi) = \frac{v du - u dv}{v^2} \quad (\text{B.9})$$

where

$$du = \sin\theta$$

$$dv = \frac{L_1^* - [r_o^* \cos\theta + S_4^* \sin\theta]}{v}$$

The view factor between two infinitesimal segments is given by  
(see Ref 8, Eq.(36))

$$F_{1 \rightarrow \zeta} = \frac{1}{2} \frac{d(\sin\psi)}{d\zeta} d\zeta \quad (\text{B.10})$$

Combining Eqs.(B.1), (B.9), and (B.10) and noting that increasing  $\zeta$  corresponds to decreasing  $\psi$  yields

$$F_{1 \rightarrow \zeta} = \frac{1}{2} \frac{[r_o^* \sin\theta - t^*][L_1^* \cos\theta - t^*]}{Z^{3/2}} d\zeta \quad (\text{B.11})$$

where

$$Z = L_1^{*2} - 2L_1^* [r_o^* \cos\theta + t^* \tan\theta] + r_o^{*2} + \left[\frac{t^*}{\cos\theta}\right]^2$$



and

$$L_1^* = [r_o^{*2} - t^{*2}]^{1/2} + \zeta + t^* \tan \theta$$

The view factor,  $F_{1 \rightarrow \zeta}(1,1)$ , from the first heatpipe condenser surface segment ( $r_o^* \Delta \theta / 2$ ) to the immediately adjacent fin segment ( $\Delta \zeta / 2$ ) cannot be evaluated with Eq.(B.11). To evaluate this view factor, the first heatpipe condenser segment was assumed to be located at a distance along the heatpipe condenser of  $r_o^* \Delta \theta / 4.75$  away from the fin and the first fin segment was assumed to be located at a distance along the fin of  $\Delta \zeta / 5.0$ . The view factor,  $F_{\zeta \rightarrow 1}(1,1)$ , is then defined so that the sum of all the view factors, from the fin segments to the point on the heatpipe condenser at a distance  $r_o^* \Delta \theta / 4.75$  from the fin, is equal to the value that would be obtained for the view factor from the fin, as a single surface, to the same point.

The error in replacing the continuous fin-heatpipe condenser surface by finite segments was evaluated by adding all the view factors to a given point and comparing the result to the analytical expression for the view factor. The maximum error was approximately 1.5 percent which indicates good results with a negligible error since there are 100 fin segments.

## B.2 View Factor from Pipe to Pipe[3]

The geometry of the problem for evaluating the view factor from heatpipe to heatpipe is shown in Fig.B.2 and the parameters are expressed in the non-dimensional terms which was divided by the half of fin length,  $L$ .

Geometric identities :

$$\psi = \theta_1 + \delta \quad (B.12)$$

$$\sin \delta = \frac{a^*}{c^*} \quad (B.13)$$

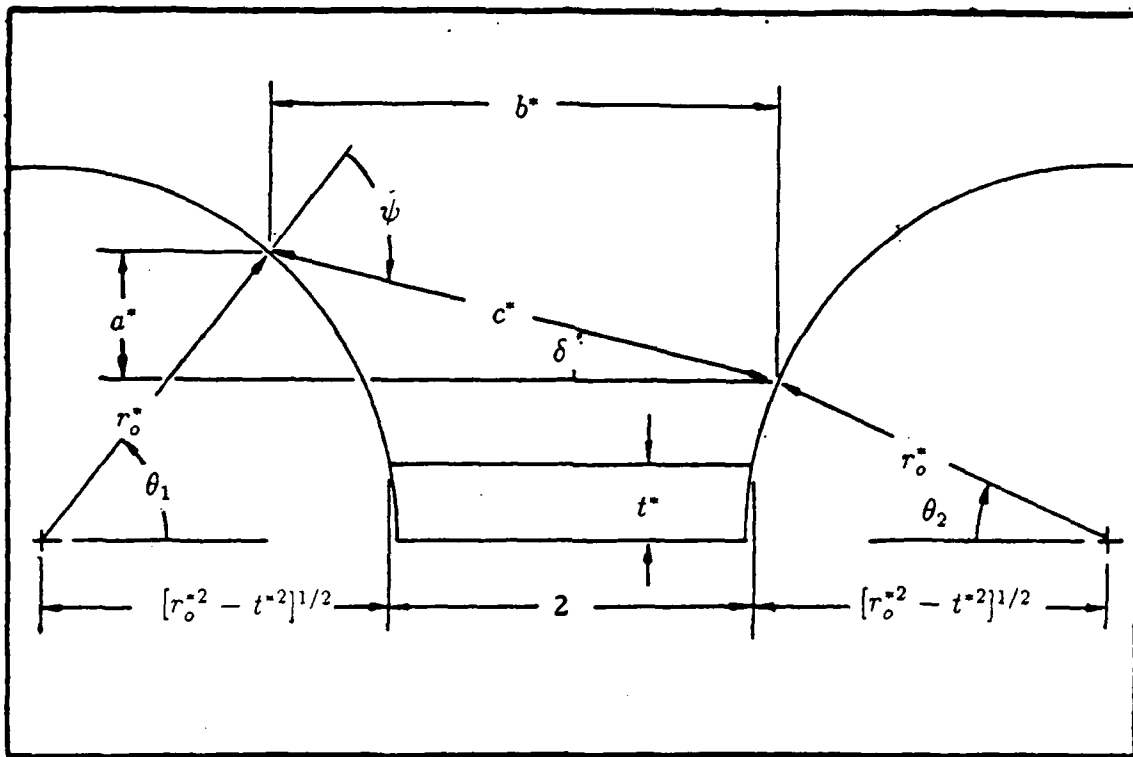


Figure B.2. Geometry Used in Heatpipe-to-Heatpipe View Factor Determination

$$\cos \delta = \frac{b^*}{c^*} \quad (\text{B.14})$$

$$a^* = r_o^* [\sin \theta_1 - \sin \theta_2] \quad (\text{B.15})$$

$$b^* = 2[1 + \{r_o^{*2} - t^{*2}\}^{1/2}] - r_o^* [\cos \theta_1 + \cos \theta_2] \quad (\text{B.16})$$

$$c^{*2} = a^{*2} + b^{*2} \quad (\text{B.17})$$

From Eq.(B.12)

$$\cos \psi = \cos \theta_1 \cos \delta - \sin \theta_1 \sin \delta \quad (\text{B.18})$$

From Eq.(B.10)

$$F_{2 \rightarrow 1} = \frac{1}{2} \cos \psi \frac{d\psi}{d\theta_2} d\theta_2 \quad (\text{B.19})$$

From Eq.(B.12), (B.13), and (B.14)

$$\frac{d\psi}{d\theta_2} = \frac{d}{d\theta_2} \left( \tan^{-1} \frac{a^*}{b^*} \right) \quad (\text{B.20})$$

Performing the differentiation of Eq.(B.20) becomes

$$\frac{d\psi}{d\theta_2} = \frac{b^* \frac{da^*}{d\theta_2} - a^* \frac{db^*}{d\theta_2}}{c^{*2}} \quad (\text{B.21})$$

where

$$\frac{da^*}{d\theta_2} = -r_o^* \cos\theta_2$$

and

$$\frac{db^*}{d\theta_2} = r_o^* \sin\theta_2$$

Combining Eq.(B.13),(B.14), and (B.18) yields

$$\cos\psi = \frac{b^* \cos\theta_1 - a^* \sin\theta_1}{c^*} \quad (\text{B.22})$$

Combining Eq.(B.19),(B.21), and (B.22) yields

$$F_{2 \rightarrow 1} = \frac{[b^* \cos\theta_1 - a^* \sin\theta_1][b^* \cos\theta_2 - a^* \sin\theta_2]}{[a^{*2} + b^{*2}]^{3/2}} \frac{r_o^* d\theta}{2} \quad (\text{B.23})$$

where

$$a^* = r_o^* [\sin\theta_1 - \sin\theta_2]$$

and

$$b^* = 2[1 + \{r_o^{*2} - t^{*2}\}^{1/2}] - r_o^* [\cos\theta_1 + \cos\theta_2]$$

Appendix C. *TABULATED RESULTS*

Table C.1. Characteristics of Radiator Parameter vs Condenser Temperature

$T_v$	Conductivity	$\beta_1$
-----	-----	-----
300.00	401.8	0.00038
320.00	400.4	0.00046
340.00	396.3	0.00056
360.00	393.8	0.00067
380.00	391.6	0.00079
400.00	389.5	0.00093
420.00	387.5	0.00108

Table C.2. Characteristics of temperature Difference and total heat transfer rate vs. Operating Temperature

$T_v$	$Q_{total}$	$T_{pe} - T_{pc}$
-----	-----	-----
300.00	166.71	6.814
320.00	201.73	7.187
340.00	241.76	8.349
360.00	278.23	9.693
380.00	338.60	11.253
400.00	396.35	13.067
420.00	460.98	15.183

Table C.3. Characteristics of Heat Pipe vs. Operating Temperature

$T_v$	$U_{HP,p}$	$\eta_{eff}$
300.00	54914.8	0.9722
320.00	57177.4	0.9088
340.00	58992.6	0.8546
360.00	60364.8	0.8076
380.00	61297.2	0.7672
400.00	61792.2	0.7315
420.00	61851.5	0.7000

Table C.4. Characteristics of Black Surface Heatpipe Radiators with Fins of Negligible Thickness

$$t^* = 0.001 \quad \epsilon_p = \epsilon_f = 1.0$$

$$r_o^* = 1.0$$

Beta	midpt Temp	Efficiency (fin)	Efficiency (eff)
10.0	0.636	0.130	0.723
5.0	0.676	0.190	0.747
2.0	0.751	0.302	0.793
1.0	0.815	0.408	0.836
0.5	0.874	0.522	0.882

$$r_o^* = 0.6$$

10.0	0.580	0.145	0.600
2.0	0.726	0.332	0.702
0.5	0.864	0.567	0.832

$$r_o^* = 0.4$$

10.0	0.545	0.155	0.505
2.0	0.712	0.352	0.633
0.5	0.858	0.594	0.793

Appendix D. *SIMPLE FIN SOLUTION*

The characteristics of a simple fin with no incident irradiation were computed using

$$\frac{dT^*}{dx^*} = \left[\frac{2}{5}\beta\right]^{\frac{1}{2}}[T^{*5} - T_E^{*5}]^{\frac{1}{2}} \quad (\text{D.1})$$

The fin efficiency is given by

$$\eta_o = \frac{1}{\beta} \frac{dT^*}{dx^*} \Big|_{x^*=0} \quad (\text{D.2})$$

Equation(D-1) was solved by iteration. The iterations were terminated when the two computed edge temperatures(  $T_E$  ) were within  $5 \times 10^{-7}$ . The dimensionless length of the fin segment was equal to 0.005. The results are given in Table D.1. The relation between the edge temperature(  $T_E$  ) and the radiation parameter( $\beta$  ) can be expressed by the following polynomial:

$$\begin{aligned} T_E = & 0.959 - 0.223\beta + 4.641 \times 10^{-2}(\beta)^2 - 14.347 \times 10^{-3}(\beta)^3 \\ & + 1.722 \times 10^{-4}(\beta)^4 - 2.200 \times 10^{-6}(\beta)^5 \end{aligned} \quad (\text{D.3})$$



Table D.1. Characteristics of Simple Fin Radiators

Beta	midpt Temp	Efficiency
40.0	0.335	0.010
20.0	0.407	0.141
10.0	0.487	0.197
4.0	0.603	0.303
2.0	0.693	0.410
1.0	0.778	0.535
0.40	0.871	0.706
0.20	0.923	0.815
0.10	0.956	0.895
0.04	0.981	0.958

## Appendix E. *PROPERTIES*

This appendix shows the experimented data selected from reference 18 and the estimated data calculated by the least square method. The error of all properties between the experimened data and the estimated data lies within maximum 1.7 % in the operating temperature rang ( 200 - 500 K ).

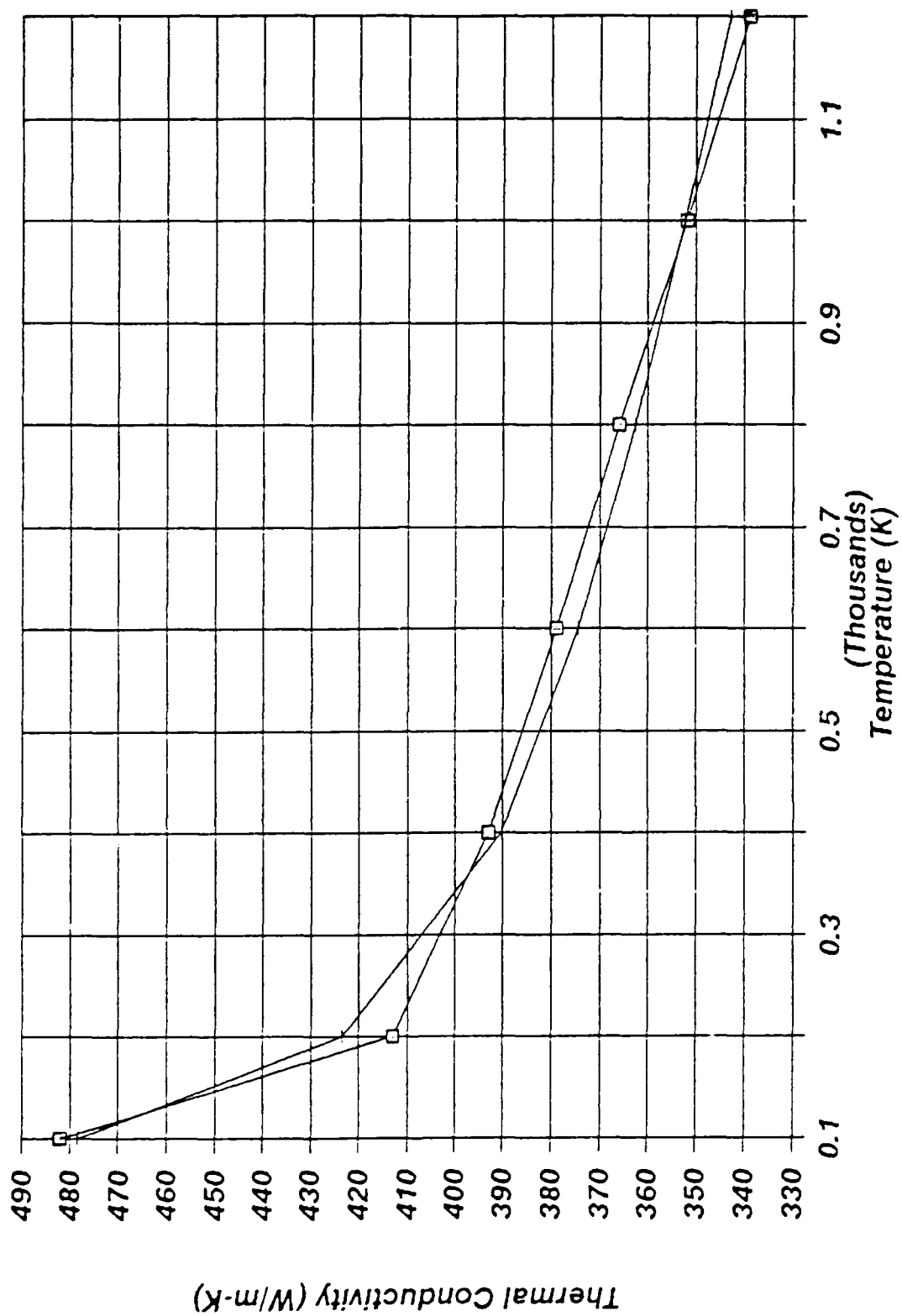


Figure E.1. Thermal Conductivity of Pure Copper

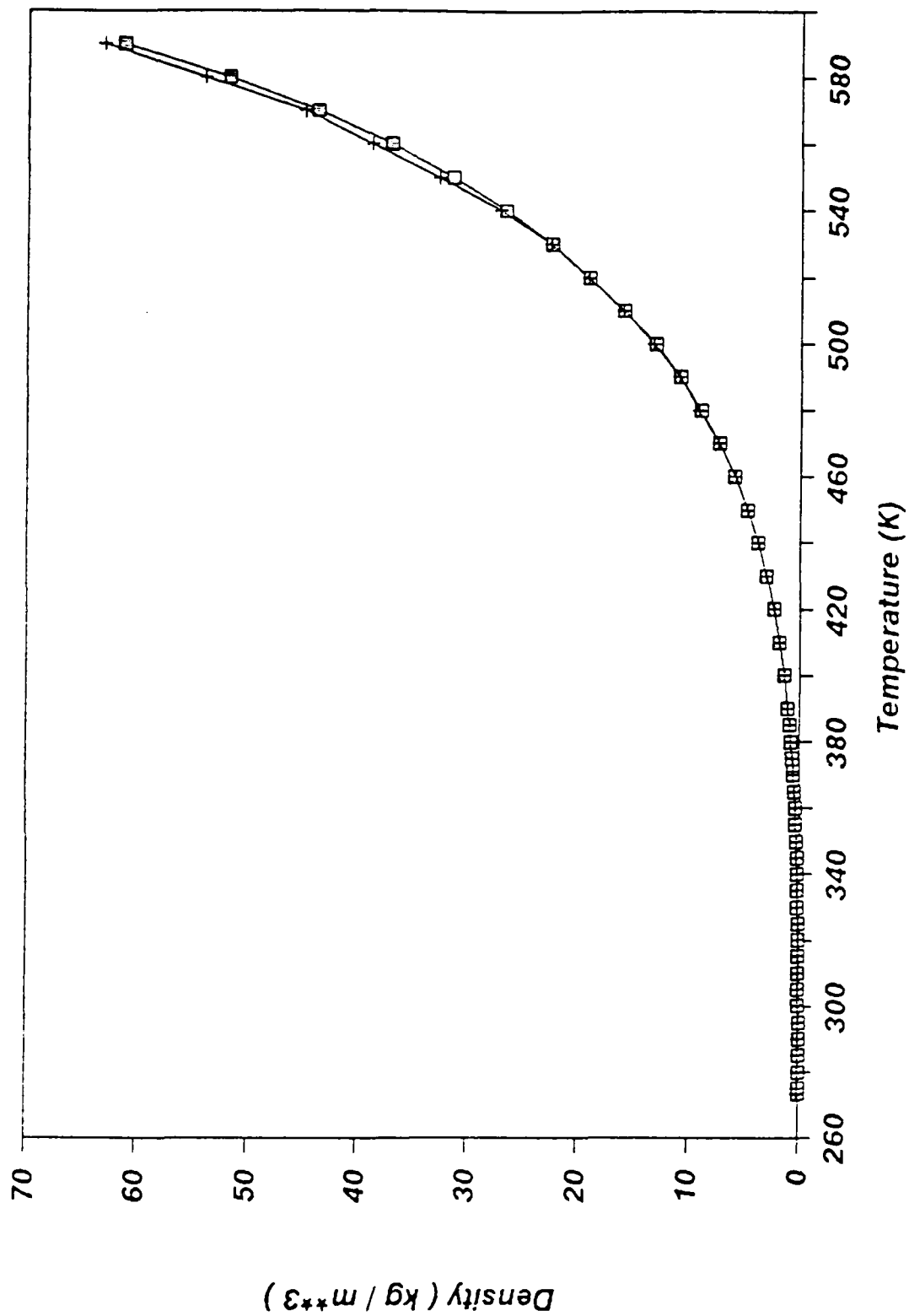


Figure E.2. Density of Saturated Water ( Steam )

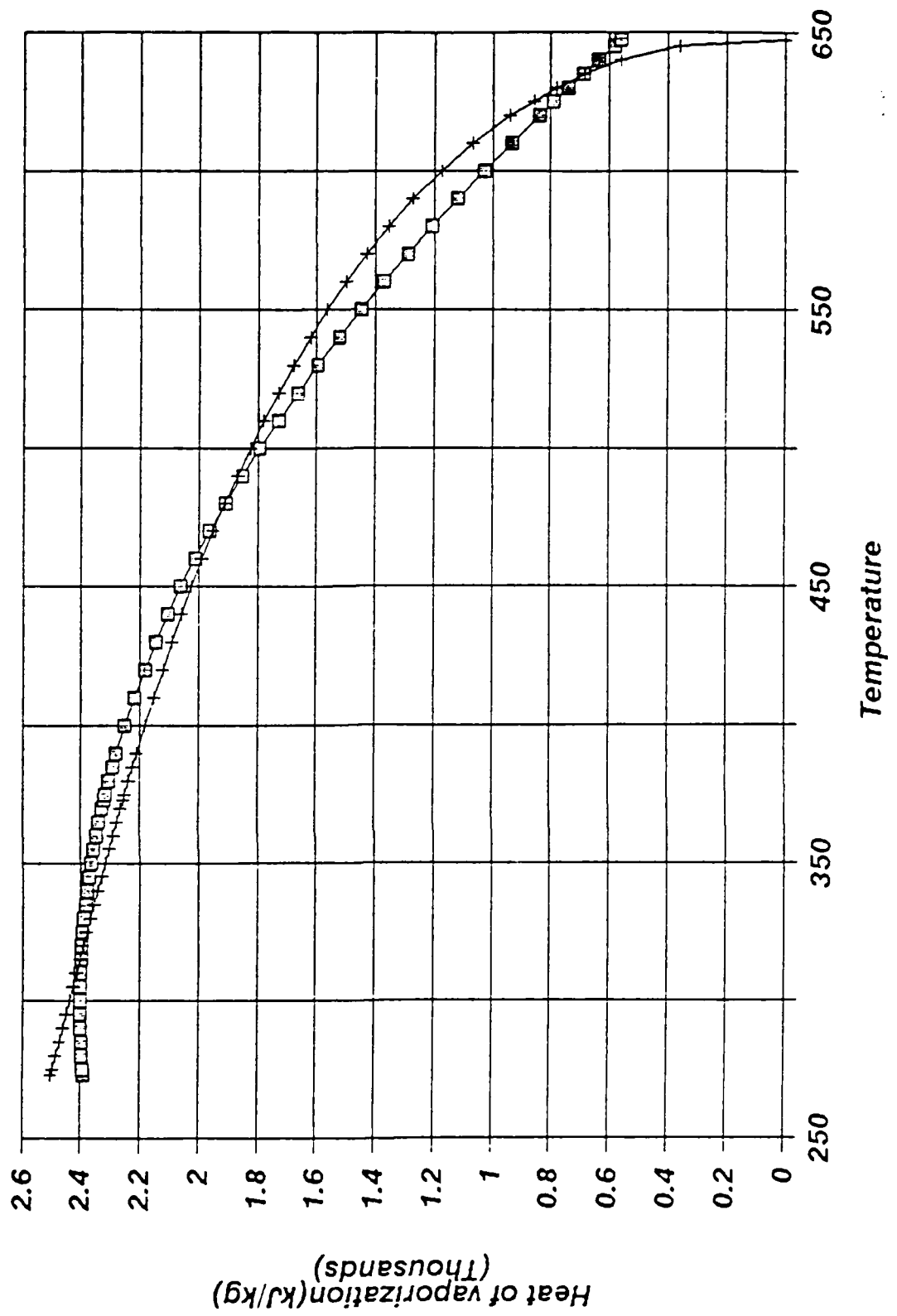


Figure E.3. Latent Heat of Vaporization ( Water )

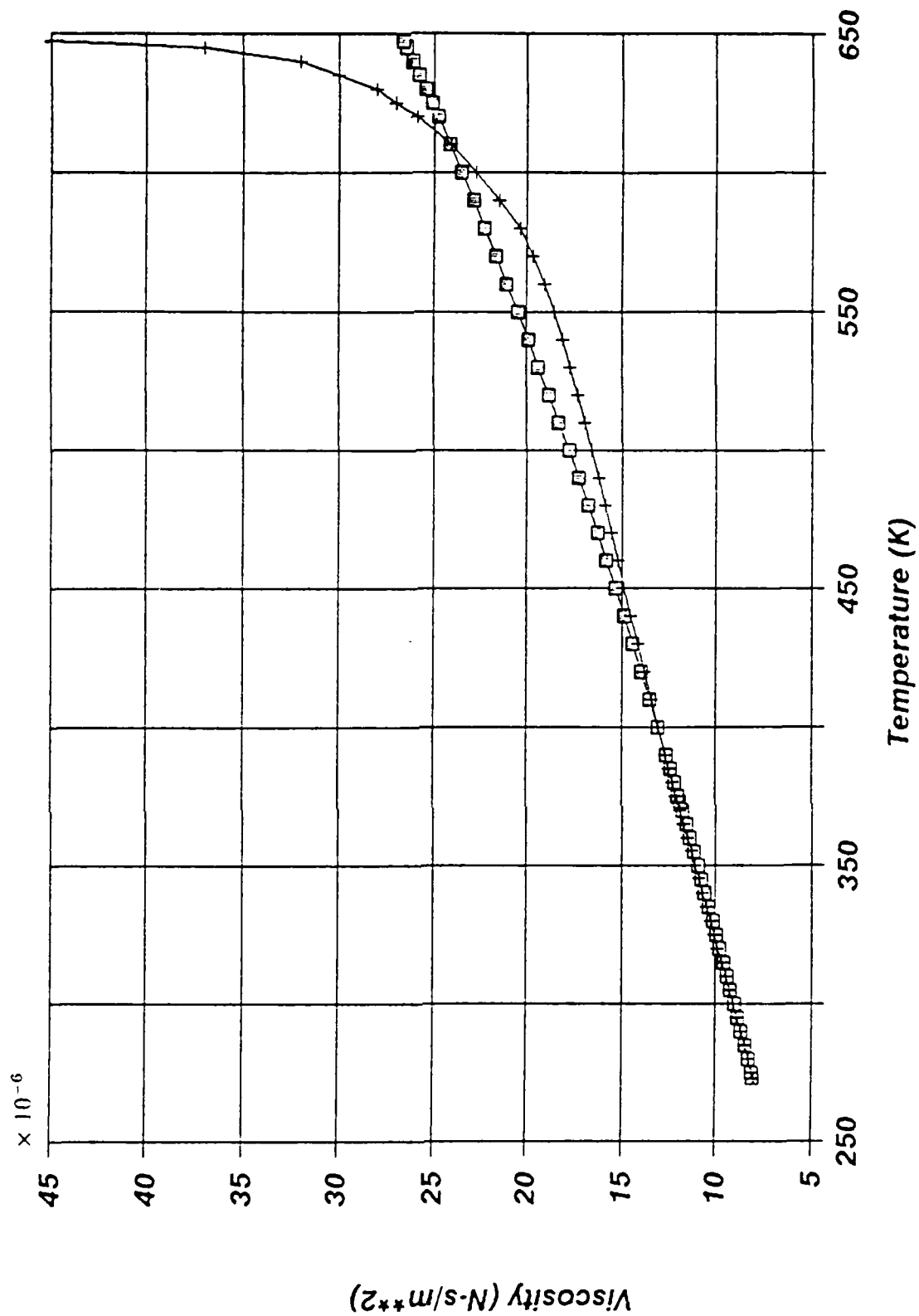


Figure E.4. Viscosity of Water ( Steam )

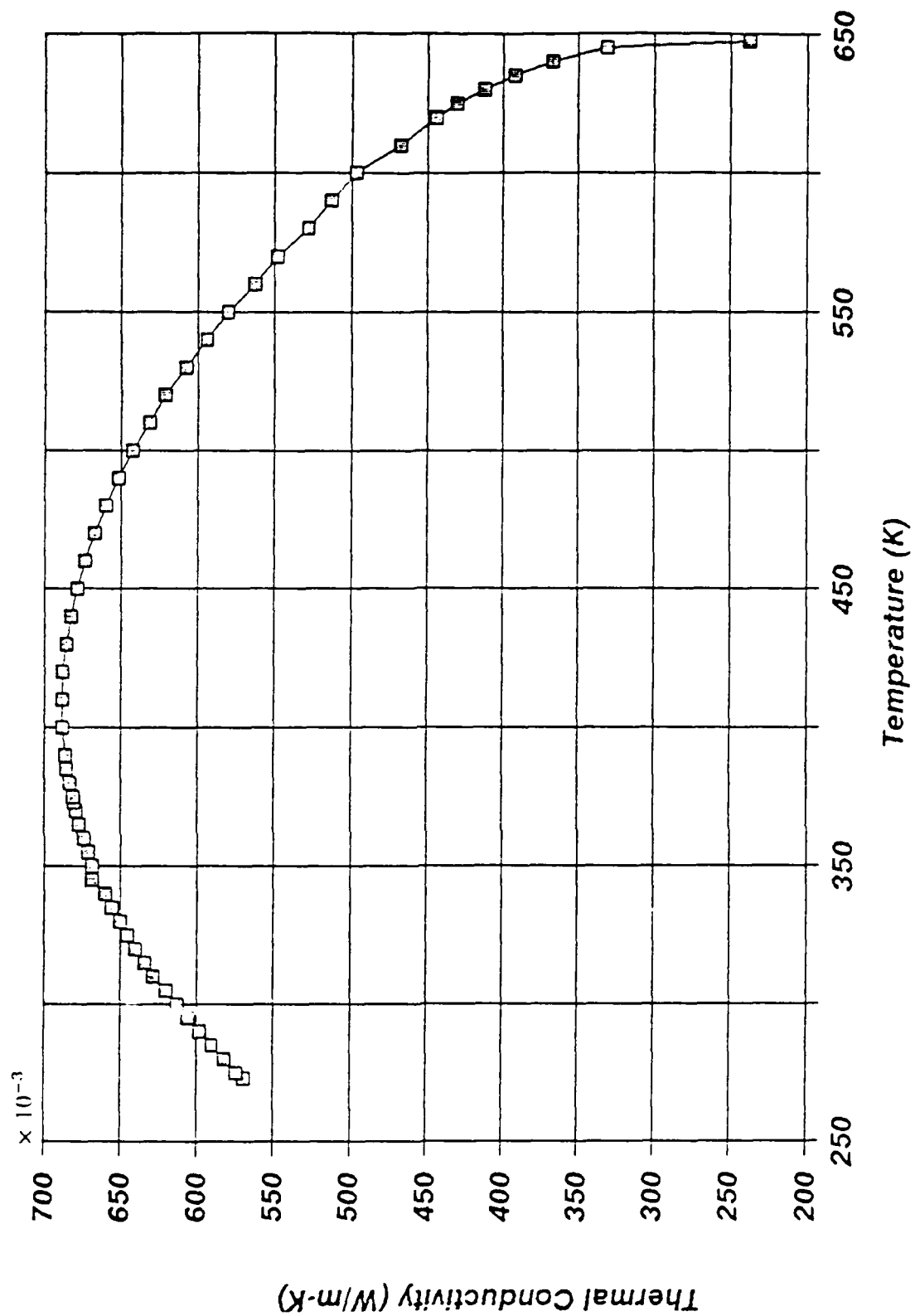


Figure E.5. Thermal Conductivity of Water ( Liquid )

## Bibliography

1. Bartas, J. G. and Sellers, W. H., "Radiation Fin Effectiveness," *Journal of Heat Transfer*, Vol.82, pp.73-75, February 1960.
2. Chi, S. W., *Heat Pipe Theory and Practice*, Hemisphere Publishing Corporation, Washington, D.C., 1976.
3. Daws, O.F., "The Emissivity of the Groove," *British Journal of Applied Physics*, Vol.5, pp. 182-197, May 1954.
4. Dunn, P. D. and Reay, D. A., *Heat Pipe*, 3rd edition, Pergamon Press, Elmsford, N.Y., 1982.
5. Eckert, E.R.G., Irvine, T.F., Jr., and Sparrow, E.M., "Analytic Formulation for Radiating Fins with Mutual Irradiation," *ASR Journal*, Vol.30, No.7, pp. 644-646, July 1960.
6. English, R.E. and Guentert, D.C. "Segmenting of Radiators for Meteoroid Protection." *ASR Journal*, Vol.31, No.8 pp 1162-1164, August 1961.
7. Heaslet, M. A. and Lomax, H., "Numerical Predictions of Radiative Interchange between Conducting Fin with Mutual Irradiations," *NASA TR R-166*, Washington, D.C., 1961.
8. Hottel, C.H., *Radiant Heat Transmission*, McGraw-Hill, 3rd edition, N.Y., 1954.
9. Jacob, M., *Heat Transfer*, Vol. 2, John Wiley & Sons, Inc., New York, N.Y., 1957.
10. Lieblin, S., "Analysis of Temperature Distribution and Radiant Heat Transfer Along a Rectangular Fin of Constant Thickness," *NASA TN D-196*, Washington, D.C., November, 1959.
11. Rubin, I. and Imber, M., "Optimization Study of Space Radiators," *AIAA Journal*, Vol.2, No.2, pp. 353-358, February 1964.
12. Sarabia, M.F. and Hitchcock, J.E., "Heat Transfer from Gray Fin-Tube Radiators," *Journal of Heat Transfer*, Vol.88, pp. 338-341, 1966.
13. Sparrow, E. M. and Eckert, E. R. G., "Radiant Interaction between Fin and Base Surfaces," *Journal of Heat Transfer*, pp. 12-18, February 1962.
14. Sparrow, E. M., Eckert, E.R.G., and Irvine, T.F., Jr., "The Effectiveness of Radiating Fins with Mutual Irradiation," *Journal of Aerospace Sciences*, Vol.28, pp. 763-772, 1961.



15. Sparrow, E.M., Miller, G.B., and Johnson, V.K., "Radiating Effectiveness of Annular-Finned Space Radiators, Including Mutual Irradiation Between Radiator Elements," *Journal of the Aerospace Sciences*. Vol.29, No.11, pp. 1291-1299, November 1962.
16. Stockman, N. O. and Kramer, J. L., "Effect of Variable Thermal Properties on One-Dimensional Heat Transfer in Radiating Fins," *NASA TN D-1878*, Washington, D.C., October 1963.
17. Tatom, J. W., "Steady-State Behavior of Extended Surfaces in Space," *ASR Journal*, Vol.30, pp. 118, 1960.

## *Vita*

Chul Hwan Yang [REDACTED], [REDACTED]

[REDACTED], the son of Jung-Suk and Jung-Ok Yang. After graduating from Chung-Dong high school in Seoul, he attended the Korean Air Force Academy. In March 1981, he graduated with the degree of Bachelor of Science in Aeronautical Engineering from the Korean Air Force Academy. Upon graduation from the Air Force Academy he received his commission as Lieutenant in the ROKAF and attended Pilot Training School. After completing pilot training he has served as a fighter pilot in the Korea Tactical Fighter Wing. He also served as a tactics operation officer in the Operations Division and served as a tactics evaluation officer in the Tactics Evaluation Division of the Korean Air Force. His military assignment prior to coming to the Air Force Institute of Technology was as an instructor pilot in the Training Wing. In May 1988, he entered the School of Engineering, Air Force Institute of Technology.

[REDACTED]  
[REDACTED]  
[REDACTED]  
[REDACTED]  
[REDACTED]

## REPORT DOCUMENTATION PAGE

Form Approved  
MAY 1964 EDITION

1a REPORT SECURITY CLASSIFICATION <b>UNCLASSIFIED</b>			1b RESTRICTED MARKING <b>N/A</b>		
2a SECURITY CLASSIFICATION AUTHORITY			3 DISTRIBUTION/AVAILABILITY OF REPORT <b>APPROVED FOR PUBLIC RELEASE DISTRIBUTION UNLIMITED</b>		
2b DECLASSIFICATION/DOWNGRADING SCHEDULE					
4 PERFORMING ORGANIZATION REPORT NUMBER(S) <b>AFIT/GA/ENY/90J-02</b>			5 MONITORING ORGANIZATION REPORT NUMBER(S)		
6a NAME OF PERFORMING ORGANIZATION <b>School of Engineering</b>	6b OFFICE SYMBOL (If applicable) <b>AFIT/ENY</b>	7a NAME OF MONITORING ORGANIZATION			
6c ADDRESS (City, State, and ZIP Code) <b>Air Force Institute of Technology (AU) Wright-Patterson AFB OH 45433-6583</b>		7b ADDRESS (City, State, and ZIP Code)			
8a NAME OF FUNDING/SPONSORING ORGANIZATION <b>WRDC</b>	8b OFFICE SYMBOL (If applicable) <b>POOS-3</b>	9 PROCUREMENT INSTRUMENT IDENTIFICATION NUMBER			
8c ADDRESS (City, State, and ZIP Code) <b>WPAFB, Ohio 45433 Attn: Dr. Chang</b>		10 SOURCE OF FUNDING NUMBERS			
		PROGRAM ELEMENT NO	PROJECT NO	TASK NO	WORK UNIT ACCESSION NO
11. TITLE (Include Security Classification) (UNCLASSIFIED) <b>THERMAL ANALYSIS OF HEAT PIPE RADIATORS WITH A RECTANGULAR GROOVE WICK STRUCTURE</b>					
12. PERSONAL AUTHOR(S) <b>CHUL HWAN YANG, Major, ROKAF</b>					
13a. TYPE OF REPORT <b>MS THESIS</b>	13b. TIME COVERED FROM _____ TO _____	14. DATE OF REPORT (Year, Month, Day) <b>1990 JUNE</b>		15. PAGE COUNT <b>83</b>	
16. SUPPLEMENTARY NOTATION					
17. COSATI CODES			18 SUBJECT TERMS (Continue on reverse if necessary and identify by block number)		
FIELD	GROUP	SUB-GROUP			
<b>20</b>	<b>13</b>		<b>Heat Pipe - Fin Radiator, Rectangular Wick Structure</b>		
19. ABSTRACT (Continue on reverse if necessary and identify by block number)					
<p>Performance of a grooved heat pipe radiator has been analyzed to determine its operating characteristics. A heat transfer analysis for the heat pipe is coupled with the analysis of the fin in this study. The effects of heat pipe operating temperature on heat flux and fin efficiency are investigated. Finite difference expressions are used for the grid system of the heat pipe wall and the fin. The heat transfer coefficient of the heat pipe radiator was determined as a function of the operating temperature level. Realistic numerical results were achieved and it was shown that the required heat flux and the temperature difference between the evaporator and condenser both increase with operating temperature.</p> <p>Also, the heat transfer coefficient increased with operating temperature up to a certain point, then began to level-off near a temperature of approximately 400°K. In addition, the overall efficiency of the heat pipe-fin arrangement decreased as the operating temperature level increased.</p>					
20 DISTRIBUTION/AVAILABILITY OF ABSTRACT <input checked="" type="checkbox"/> UNCLASSIFIED/UNLIMITED <input type="checkbox"/> SAME AS RPT <input type="checkbox"/> DTIC USERS			21 ABSTRACT SECURITY CLASSIFICATION <b>UNCLASSIFIED</b>		
22a NAME OF RESPONSIBLE INDIVIDUAL <b>Capt Daniel B. Fant, Instructor, AFIT</b>			22b TELEPHONE (Include Area Code) <b>(513) 255-3517</b>		22c OFFICE SYMBOL <b>AFIT/ENY</b>